

**TDESIGN AND DEVELOPMENT
OF MODULAR RC PLANE FOR
INFLIGHT MULTITASKING
OPERATIONS**



Session: BE. Spring 2024

Project Supervisor: Adnan Maqsood

Submitted By

Amanullah

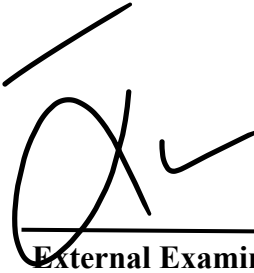
Syed Oasaja Hassan

School of Aerospace and Mechanical Engineering

**College of Aeronautical Engineering, NUST,
Risalpur**

Certification

This is to certify that **Amanullah, 326688** and Syed **Oasaja Hassan, 326660** have successfully completed the final project [**Design and Development of Modular RC Plane for Inflight Multitasking Operations**], at the **College of Aeronautical Engineering, Risalpur**, to fulfill the partial requirement of the degree **BE Aerospace**.



External Examiner

Muhammad Jamil

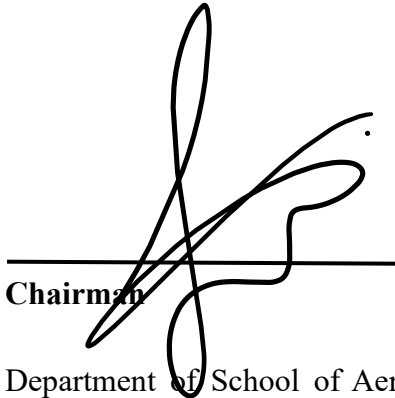
Associate Professor



Project Supervisor

Adnan Maqsood

Associate Professor



Chairman

Department of School of Aerospace and Mechanical Engineering, College of Aeronautical Engineering, NUST, Risalpur

Abstract

A compelling narrative is unfolded within the airborne realm by our project, addressing the escalating challenges posed by disruptive technologies in the UAV domain. In response to the rise of electronic jamming and hunter drone weaponry, a pioneering solution is presented - a modular RC cargo plane harboring a concealed mini aircraft with foldable wings, aptly named the counter-counter UAV. Inspired by ongoing conflicts and driven by the imperative for technological advancements, an affordable yet superior UAV is birthed through collaboration with academia. Established aerospace design methodologies such as Raymer and Roskam approaches are leveraged, combining cost-efficiency with cutting-edge capabilities in our UAV. Central to the design is the integration of a foldable wing system, enhancing transportability and adaptability across diverse mission profiles. Powered by servo motors, these wings and control surfaces ensure precise and reliable functionality. Construction prioritizes lightweight materials like Depron, reinforced with balsa wood, balancing strength with cost-effectiveness. This approach streamlines production and accelerates iterative design phases. Validation of the UAV's performance spans comprehensive testing methodologies. Computational Fluid Dynamics (CFD) simulations and wind tunnel tests assess theoretical aerodynamics, complemented by extensive real-world flight tests. These measures affirm the UAV's aerodynamic efficiency and operational suitability. A significant advancement in cost-effective, multitasking UAVs is marked by our project, poised to address both academic and practical needs in today's dynamic global landscape. With keywords including

Keywords: UAV; multitasking; inflight; CFD; wind tunnel testing; foldable wings; and aerospace design; innovation at the intersection of technology; aviation is exemplified by our endeavor.

Undertaking

I certify that the project **Design and Development of Modular RC Plane for Inflight Multi-Tasking Operations** is our own work. The work has not, in whole or in part, been presented elsewhere for assessment. Where material has been used from other sources it has been properly acknowledged/ referred.



Amanullah

326688



Syed Oasaja Hassan

326660

Acknowledgement

We truly acknowledge the cooperation and help make by **Adnan Maqsood, Associate Professor of College of Aeronautical Engineering, NUST, Risalpur**. He has been a constant source of guidance throughout the course of this project. We would also like to thank **Adnan Maqsood, Associate Professor of College of Aeronautical Engineering, NUST, Risalpur** for his help and guidance throughout this project.

We are also thankful to our friends and families whose silent support led us to complete our project.

Table of Contents

1	INTRODUCTION	xi
1.1	Project Title.....	xi
1.2	Project Description.....	xi
1.3	Project Scope	xi
1.4	Project Overview	xii
2	LITERATURE REVIEW	xii
2.1	Introduction to CC-UAV Drones.....	xii
2.2	Key Features of Drones	xii
2.2.1	Man-portability and Foldable Design	xiii
2.2.2	Manual Operation and Radio Communication	xiii
2.2.3	Low Altitude Operation and Radar Avoidance	xiii
2.2.4	Real-time Video Feed and Target Tracking.....	xiii
2.2.5	Suicidal Nature and Explosive Warhead	xiii
2.2.6	Integration of Avionics and Autonomous Systems	xiii
2.2.7	Precise Targeting and Guidance	xiii
2.2.8	Enhanced Mission Flexibility	xiii
3	Design of the UAV	xiv
3.1	Conceptual Design	xiv
3.2	Mission Requirements:	xiv
3.3	Reference Aircraft.....	xv
3.4	Design Requirements:	xvi
3.5	Weight Build Up.....	xvi
3.6	Configuration Selection:	xvii
3.6.1	T/W and W/S selection:	xviii
3.6.2	Airfoil Selection:.....	xviii
3.7	Sizing Calculations and Analysis:	xxii
3.7.1	Wing Geometry parameters:	xxii
3.7.2	Horizontal Tail Geometry parameters:	xxiii
3.7.3	Vertical Tail geometry parameters:	xxiii
3.8	Final Design Parameters	xxiii
3.9	Propulsion System	xxiii
3.10	Stability Analysis.....	xxix

3.11	Static Stability Analysis using XFLR:.....	xxix
3.11.1	Aircraft Geometry:.....	xxix
3.11.2	Trim Aircraft for Steady-State Flight:.....	xxix
3.11.3	Perform Static Stability Analysis:.....	xxix
3.11.4	Review Static Stability Results:.....	xxix
3.12	Dynamic Stability Analysis using XFLR:.....	xxx
3.12.1	Define Aircraft Configuration:.....	xxx
3.12.2	Create a Flight Dynamics Model:.....	xxx
3.12.3	Perform Time-Domain Simulation:.....	xxx
3.12.4	Analyze Dynamic Response:.....	xxx
3.12.5	Optional: Eigenvalue Analysis for Modes of Motion:.....	xxx
3.12.6	Additional Tips:.....	xxx
3.12.7	CG Estimation.....	xxx
3.12.8	XFLR V5 Setup:.....	xxxiii
3.12.9	Static Stability Analysis.....	xxxiii
3.12.10	Dynamic Stability Analysis.....	xxxv
3.12.11	Static Stability Analysis after Release.....	xxxvii
3.13	Performance Analysis.....	xliv
4	Folding Mechanism.....	lii
4.1	Torsional Spring.....	liii
4.1.1	Reason Of Failure:.....	liii
4.2	Loaded Spring.....	liii
4.2.1	Reason of Failure.....	liii
4.3	Spur Gear.....	liii
4.3.1	Reason of Success.....	liii
4.4	Servo Operated Mechanism.....	liv
4.4.1	Reason of Success.....	liv
5	Final CAD.....	liv
5.1	Introduction to CAD Modelling using SolidWorks:.....	liv
5.2	Understanding SolidWorks Interface:.....	lv
5.2.1	User Interface Overview:.....	lv
5.2.2	Parametric Modelling in SolidWorks:.....	lv
5.2.3	Sketching and Feature-Based Modelling:.....	lv
5.3	Creating 3D Models in SolidWorks:.....	lvi

5.3.1	Sketching and Constraints:	lvi
5.3.2	Extrusions and Revolves:.....	lvi
5.3.3	Fillets and Chamfers:	lvi
5.4	Assembly Modelling:.....	lvi
5.4.1	Creating Assemblies:	lvi
5.4.2	Mate Relationships:	lvi
5.4.3	Motion Studies and Simulations:.....	lvi
5.5	Surface Modelling and Complex Geometry:	lvi
5.5.1	Surface Modelling Techniques:	lvi
5.5.2	Importing and Editing Surface Geometry:.....	lvii
5.6	Detailing and Drawing Creation:	lvii
5.6.1	Creating 2D Drawings:	lvii
5.6.2	Bill of Materials (BOM) and Exploded Views:.....	lvii
5.7	Rendering and Visualization:.....	lvii
5.7.1	Photorealistic Rendering:.....	lvii
6	Prototype Development	lxi
7	Flight Testing	lxv
8	Challenges and Possible reasons.....	lxvii
9	Flights after applying correction.....	lxviii
10	Multitasking Operations.....	lxix
10.1	Deception	lxix
10.2	Reconnaissance	lxx
10.3	Suicide drone.	lxxi
10.4	Cargo drone.....	lxxii
11	CONCLUSIONS AND FUTURE WORK	lxxiii
11.1	Conclusion	lxxiii
11.2	Future Work.....	lxxiv

List of Figures

Figure 1	Design Wheel	xiv
Figure 2	Mission Profile	xv
Figure 3:	E-Flite E-130	xvi
Figure 4	Clark Y Airfoil	xix
Figure 5	Airfoil Drag Polar.....	xix

Figure 6 Airfoil Lift curve slope.....	xx
Figure 7 Aerodynamics Efficiency versus Angle of attack.	xx
Figure 8 Drag Coefficient vs Angle of Attack.....	xxi
Figure 9 Pitching Moment Coefficient versus Angle of Attack	xxii
Figure 10: Settings for Daughter plane.	xxiv
Figure 11: Motor selection for Daughter plane.....	xxiv
Figure 12: Without Daughter plane.	xxv
Figure 13: Performance without Daughter plane.....	xxv
Figure 14: Daughter Plane Propulsion.	xxvi
Figure 15: Daughter Plane Performance.	xxvii
Figure 16: With Daughter plane motor calculation.	xxviii
Figure 17: With daughter performance.	xxviii
Figure 18 Motor Selected: GT-2820-05	xxix
Figure 19: Set up for CG calculation.	xxxi
Figure 20: CG visualization in Parent plane.	xxxii
Figure 21 XFLR5 Model and Masses	xxxiii
Figure 22 Pitching Moment Coefficient versus AOA Before release.	xxxiv
Figure 23 Rolling Moment Coefficient vs Side Slip angle.....	xxxiv
Figure 24 Yawing Moment Coefficient vs Side slip angle.....	xxxv
Figure 25 Longitudinal Dynamic Stability Root Locus.....	xxxvi
Figure 26 Lateral Dynamic Stability Root Locus	xxxvii
Figure 27 Pitching Moment Coefficient versus AOA after release.	xxxviii
Figure 28 Rolling Moment Coefficient versus AOA after release.	xxxix
Figure 29 Yawing Moment Coefficient versus AOA after release.....	xl
Figure 30 Longitudinal Dynamic Stability Root Locus after release.	xl
Figure 31 Lateral Dynamic Stability Root Locus after release.....	xli
Figure 32 Directional Divergence Mode	xlii
Figure 33 Dutch Roll Mode	xlii
Figure 34 Roll mode.	xliii
Figure 35 Long Period or Phugoid mode.....	xliii
Figure 36 Short Period Mode.....	xliv
Figure 37 Aircraft Drag Polar	xlv
Figure 38 Important Aerodynamic Relations vs Velocity.	xlvi
Figure 39 Thrust Required vs Velocity.....	xlvii
Figure 40 Sink rate vs Velocity.	xlviii
Figure 41 Aerodynamic Efficiency vs Velocity.	xliv
Figure 42 Power available and Power Required vs Velocity.	l
Figure 43 Hodograph for Gliding Flight.....	li
Figure 44 Wing Folding Mechanisms	liii
Figure 45: Weighted Matrix for Release Mechanism.....	liv
Figure 46 Front view of final CAD Model	lviii
Figure 47: Top View of final CAD model.....	lviii
Figure 48: Completely Folded Wings of daughter UAV.....	lix
Figure 49: Top view of daughter UAV.....	lx
Figure 50: Unfolded daughter plane.	lx

Figure 51: Inflight Separation Visualization.....	lxi
Figure 52: Fabricated Parts of Parent airplane.....	lxii
Figure 53: Control Surfaces positioning on fuselage.....	lxii
Figure 54: Parents wing.	lxiii
Figure 55:Fuselage for cargo parent airplane.	lxiv
Figure 56:Fabricated parts for daughter plane	lxiv
Figure 57: Parent plane in spin.	lxv
Figure 58: Daughter plane in Roll.	lxvi
Figure 59 Challenges faced during development.....	lxvii
Figure 60: Successful flight of Parent plane.	lxviii
Figure 61: Successful flight of daughter plane.	lxix
Figure 62: Austria HG 86 Mini.....	lxxii

INTRODUCTION

Project Title

“Design and Development of Modular RC plane for Inflight multitasking operations”.

Project Description

Amidst a world grappling with escalating conflicts and heightened security challenges, our project aims to revolutionize the aerial domain by introducing a novel approach to unmanned aviation. Focused on the design and development of a modular RC plane, featuring a cargo plane housing a mini plane with foldable wings, our initiative stands as a testament to innovation in the face of evolving warfare dynamics. This ambitious undertaking melds cutting-edge technology, advanced aerospace engineering, and meticulous testing, marking a pioneering stride in the pursuit of aerial supremacy.

Our approach leverages Depron foam paired with Balsa wood for streamlined, lightweight construction. This combination aligns with our vision for efficiency and structural integrity. This choice not only keeps production costs in check but also facilitates rapid prototyping, allowing us to iterate swiftly for optimal design refinement.

Ensuring the UAV's aerodynamic excellence is paramount. To achieve this, we harness This approach guarantees that our UAV operates at the highest levels of efficiency and precision.

{Motivation

Driven by the urgency to meet contemporary security demands, our project endeavors to make a significant contribution to cutting-edge UAV technology. Our focus centers on crafting a small, foldable-wing modular RC plane, poised to provide a solution that is both cost-efficient and adept at addressing the challenges posed by modern conflict scenarios.

My motivation also stems from the desire to collaborate with our academic institution, harnessing the expertise and resources available to us. By aligning our project with academic objectives, we aspire to bridge the gap between theoretical knowledge and practical application, fostering a holistic learning experience for ourselves and future generations of engineers and researchers.

Project Scope

Our project ambitiously aims to conceive, build, and authenticate a compact and economical two modular RC planes, designed specifically for multipurpose applications seen visually and acoustically one and will have the capability to be separated during flight in modern conflict environments. Embracing state-of-the-art technology and adhering to advanced aerospace engineering principles, our approach draws inspiration from renowned methodologies, including those proposed by Raymer and Roskam.

Integral to our methodology is the utilization of Depron foam and Balsa wood, steering away from traditional manufacturing norms for heightened efficiency and cost-effectiveness. The

project will explore potential tactical applications, intelligence gathering, and rapid deployment capabilities, aligning with the current technological landscape and real-world defense needs.

Project Overview

Chapter 1 deals with the introduction and project description. It explains the need for the project and a brief introduction to the project.

Chapter 2 presents a detailed literature review for the development of a UAV.

Chapter 3 includes the conceptual design of the UAV. It also presents Stability as well as performance analysis of the UAV.

Chapter 4 shows the development process of the Folding mechanism for the wings of Daughter UAV.

Chapter 5 presents the complete CAD model of the aircraft which was further used to manufacture the UAV.

Chapter 6 shows the process of prototype development from the CAD.

Chapter 7 includes the flight testing of the UAV.

Chapter 8 shows the challenges encountered during the project as well as the future works of the project.

Chapter 9 Successful flights

Chapter 10 shows the multitasking operation that can be done with this assembly.

Chapter 11 Conclusion and Future work

LITERATURE REVIEW

Certainly, I can provide a more structured version of the information with increased headings:

Introduction to CC-UAV Drones

In response to contemporary security challenges, Counter Counter-UAV design and development of a compact modular RC plane which can serve as a response to the counter UAV technologies in the world performing military applications getting the task done at hand in a proficient manner achieving cost effectiveness.

This paradigm shift in drone technology has been driven by the need for rapid and precise strike capabilities, particularly in scenarios where deploying conventional munitions or risking human pilots may be impractical or too risky.

Key Features of Drones

C-C UAV drones possess several distinct features that make them valuable assets on the modern battlefield. These features include:

Man-portability and Foldable Design

The design of drones emphasizes portability and ease of transport. They are engineered to be carried and deployed by an individual or a small team. Additionally, their foldable structure allows for compact storage and swift deployment, making them highly versatile in various operational environments.

Manual Operation and Radio Communication

Operators have direct control over both of drones through radio communication. This manual operation allows for real-time adjustments and decision-making based on changing battlefield conditions. It also enables operators to select specific targets and adjust flight trajectories as needed.

Low Altitude Operation and Radar Avoidance

Drones are engineered to operate at extremely low altitudes, typically just a few meters above the ground. This design choice serves a dual purpose. Firstly, it allows them to remain stealthy and undetectable by conventional radar systems. Secondly, it positions the drone for precise, low-level strikes against targets.

Real-time Video Feed and Target Tracking

Equipped with on-board cameras, drones provide live video feeds to operators. This feature is crucial for various operational tasks, including reconnaissance, intelligence gathering, and target tracking. It allows operators to maintain situational awareness and make informed decisions during missions.

Suicidal Nature and Explosive Warhead

Daughter drones are designed to be inherently suicidal in nature. Unlike parent UAV that return to base after completing their mission, Daughter drones are intended to impact their targets directly. They are armed with an explosive warhead located at the front, which detonates upon contact with the target, ensuring a high probability of mission success.

Integration of Avionics and Autonomous Systems

An essential aspect of drone development is the integration of advanced avionics and autonomous systems. This enhancement aims to achieve:

Precise Targeting and Guidance

Advanced avionics and autonomous systems work in tandem to facilitate precise targeting. These systems employ a combination of GPS coordinates, inertial guidance, and sensor data to ensure accurate navigation towards the designated target. Additionally, the integration of artificial intelligence algorithms allows for real-time adjustments to account for any changes in the operational environment.

Enhanced Mission Flexibility

The incorporation of advanced avionics significantly enhances the mission flexibility of Counter-counter UAV drones. These systems enable the drone to adapt to dynamic battlefield scenarios, allowing for multiple mission profiles within a single deployment. This adaptability is particularly crucial in situations where mission objectives may change or evolve in real-time.

Design of the UAV

Conceptual Design

The aircraft design and development can be broken down into three phases. These phases are conceptual design, preliminary design, and detailed design respectively. Conceptual design is the first, foremost, and most important design phase. In this phase, the designer analyzes the mission requirements that are to be fulfilled by the aircraft. The designer looks up the possible aircraft configurations and makes compromises on key aspects which ultimately lead to an altogether different aircraft set to fulfill the given mission requirements. The designer's main aim is to design an aircraft that, along with fulfilling the mission requirement is also affordable and easy to manufacture.

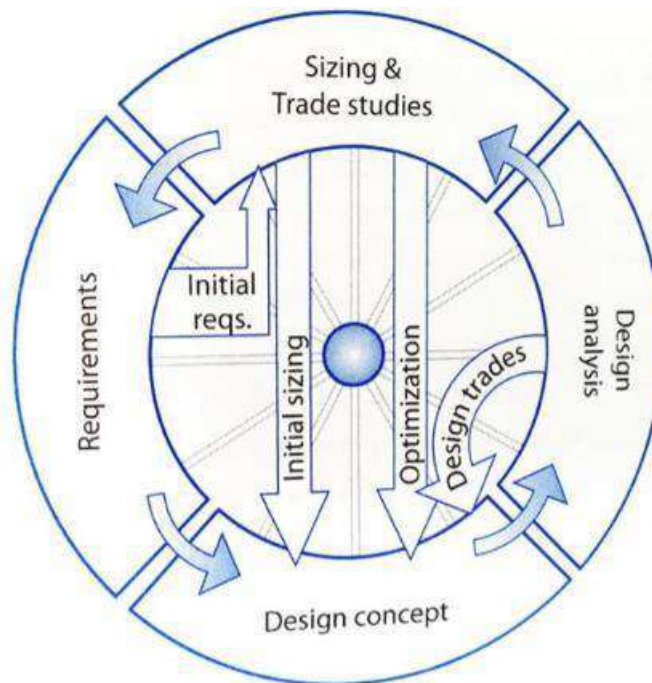


Figure 1 Design Wheel

The conceptual design is very flexible, and it keeps changing depending upon what the mission requirements dictate. Mission requirements are the first thing that a designer looks up when he starts his initial design phase. These mission requirements drive the complete process of aircraft design and multiple compromises are made to meet the set requirements. Following are brief mission requirements and design constraints for the competition.

Mission Requirements:

The mission requirements hold key importance in the design of an aircraft. Every designer looks up the mission requirements to start off the design process. The general mission requirements of the multitasking UAV are:

- Carrying another aircraft inside

- Visually and acoustically single aircraft
- Effortless Mobility: Lightweight and Portable
- Modular Design: Foldable Wings on daughter plane
- Versatile Payload Integration: Adaptable for Strap Down Cameras, or Warheads
- Live Operations, Remote Monitoring: Seamless Surveillance Solutions

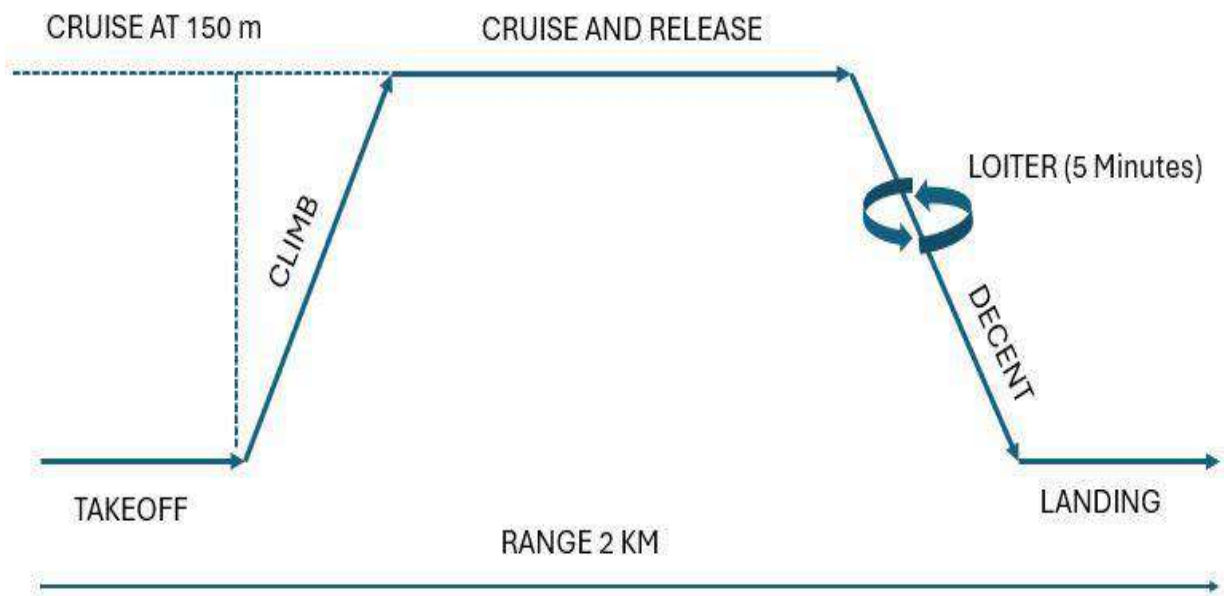


Figure 2 Mission Profile

Reference Aircraft

‘E-130’ was selected as the reference aircraft for the design of the Parent UAV.

Table 1 Reference Aircraft

Manufacturer	E-Flite
Payload	0.35 kg
Span	1.5 m
MTOW	2.7 kg
Endurance	10 min
Range	10 km
Altitude	200 m



Figure 3: E-Flite E-130

Design Requirements:

Keeping in view the given mission constraints (requirements) following are the key design requirements that must be kept in check for the successful completion of the mission:

Table 2 Design Requirements

Sr No.	Design Requirements	Value
1	Maximum Takeoff Weight	< 2.5 kg
2	Payload	0.3 kg
3	Cruise Speed	>20 m/s
4	Operating Speed	150 m AGL
5	Endurance	>5 min
6	Range	2 km

Weight Build Up

Building an RC drone involves assembling various components, each with its own weight considerations. The frame, crafted from materials like carbon fiber or aluminum, forms the structural foundation, weighing around 50-100 grams for smaller models and several hundred grams for larger ones. Motors, typically weighing 20-50 grams each, drive the propellers to generate thrust, while Electronic Speed Controllers (ESCs), ranging from 5-20 grams each, regulate motor speed. The flight controller, weighing approximately 10-30 grams, acts as the drone's brain, orchestrating stabilization and control algorithms. Power is provided by lithium polymer (LiPo) batteries, weighing 150-200 grams for a 3S 2200mAh model, while propellers contribute 10-30 grams collectively. Additional components such as the receiver (5-15 grams),

transmitter (200 grams to over 1 kilogram), and optional FPV equipment (50-100 grams for a basic setup) may also be integrated. Attention to weight distribution and balance is crucial to optimize performance and flight characteristics, with lighter components often translating to extended flight times and improved maneuverability.

Table 3 Weight Build Up

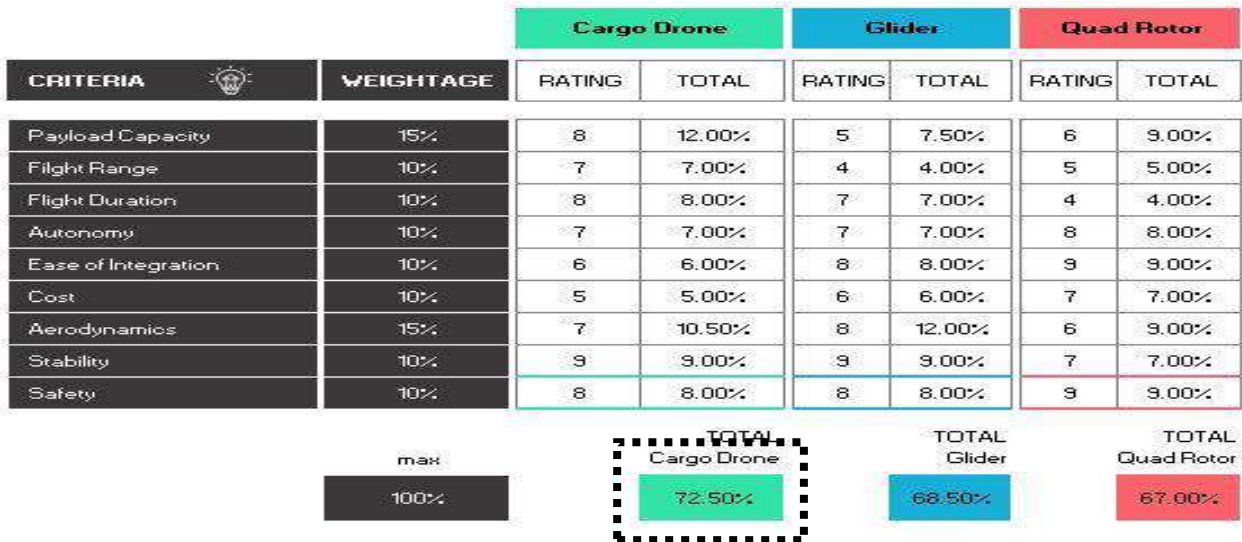
System	Component	Weight (grams)
Propulsion	GT-2820-05 (1180)	140*2= 280
	Gem fan Propeller (10x4.5 in)	15*2= 30
	Battery 2200 mAh (4s-11.1V)	84
	Skywalker 60 Amp ESE	120
Payload	-	300
UAV	Empty Structure Weight	800
Flight Control	Servo (Control Surface)	36
Total UAV Weight	-	1650 (1.65 kg)

Configuration Selection:

A High-rectangular-wing aircraft with a Swept tail was selected for the purpose of this project. A twin motor configuration was chosen based on its high payload carrying characteristics. The puller propeller is inherently unstable and vice versa.



The foldable wing aircraft was selected as daughter plane as it provides the ability to stay inside the parent aircraft. The pusher propeller was selected for daughter plane that provide space to suck air from and does not interfere with the air being used as an intake to the propulsion system.



T/W and W/S selection:

Based on the selection criteria for an RC drone typically involve achieving a balance between thrust-to-weight ratio (T/W) and wing loading (W/S) to ensure optimal performance and maneuverability. A thrust-to-weight ratio of 1.2 indicates that the drone can produce 1.2 times its weight in thrust, allowing for agile maneuvers and quick acceleration. This ratio is particularly advantageous for aerobatic flight and responsive control. Meanwhile, a wing loading of 64 W/S indicates the weight of the drone distributed over the wing area, affecting its lift capability and stall speed. With this moderate wing loading, the drone can maintain stability and lift while still being agile enough for dynamic flight maneuvers. The selection procedure involves analyzing the intended use of the drone, such as aerial photography, racing, or acrobatics, and then determining the appropriate balance between thrust-to-weight ratio and wing loading to meet performance requirements and pilot preferences. Additionally, considerations such as motor power, propeller size, frame design, and overall weight distribution play crucial roles in achieving the desired T/W ratio and W/S for the selected RC drone

Table 4 Thrust to Weight Ratio and Wing Loading Selection

T/W	1.2
W/S	64

Airfoil Selection:

When selecting an airfoil for an RC aircraft, factors such as lift characteristics, drag, stability, and maneuverability are crucial considerations. The Clark-Y airfoil is a popular choice due to its favorable lift and drag properties, making it suitable for a wide range of applications from general aviation to RC model aircraft. Utilizing tools such as Airfoil Tools provides valuable insights into the aerodynamic performance of the Clark-Y airfoil.

The Clark-Y airfoil is characterized by its relatively flat lower surface and a gently curved upper surface, which results in a favorable lift-to-drag ratio across a range of angles of attack. Airfoil Tools offers comprehensive graphical representations of the lift and drag coefficients as functions of angle of attack. These graphs allow modelers to visualize the

airfoil's performance under varying flight conditions, aiding in the selection process.

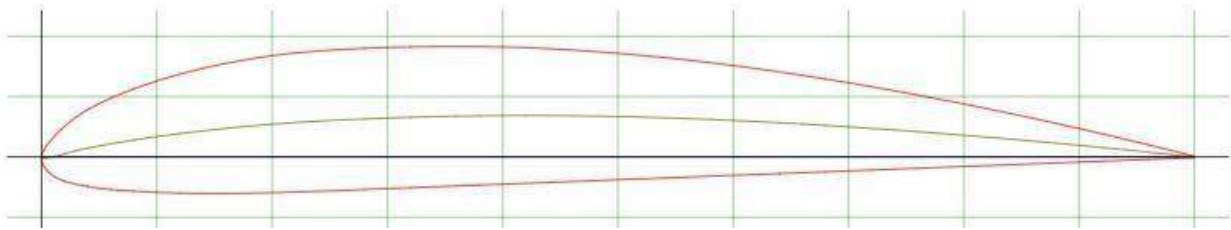


Figure 4 Clark Y Airfoil

Figure 4: Airfoil Geometry

Table 5 Comparison of Airfoils

Sr. No.	Airfoil	C_{l_0}	C_{d_0}	$C_{l_{max}}$	Stall Angle
1	NACA 2412	0.26	0.013	1.38	13.8
2	M6	0.08	0.015	1.23	11.5
3	Clark-Y	0.4	0.011	1.43	10.7

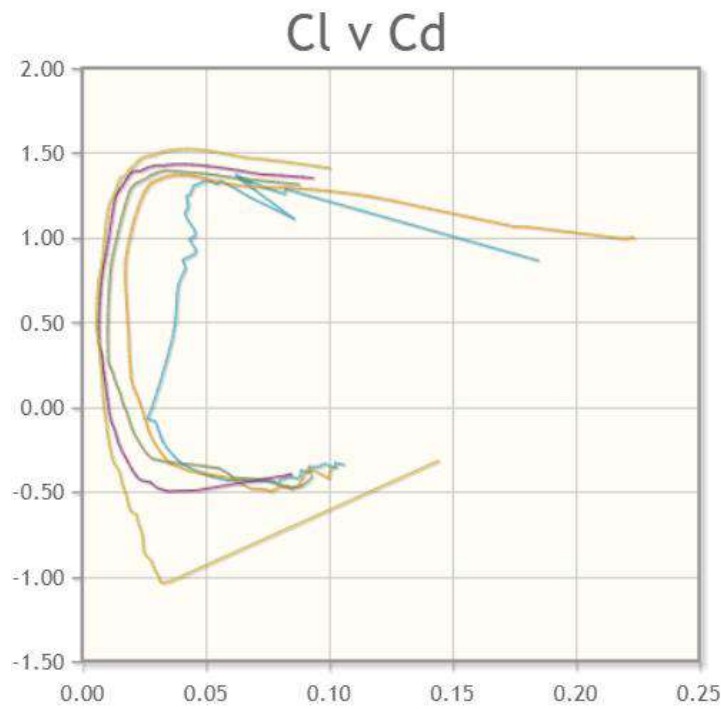


Figure 5 Airfoil Drag Polar

Analyzing the lift coefficient (C_l) versus angle of attack (α) graph reveals the airfoil's lift-producing capabilities at different angles of attack. The Clark-Y airfoil typically exhibits a gradual increase in lift coefficient with increasing angle of attack, reaching its maximum lift coefficient before experiencing stall. This characteristic ensures stable lift production during normal flight operations and allows for predictable stall behavior, making it suitable for beginner-friendly RC aircraft as well as more advanced designs.

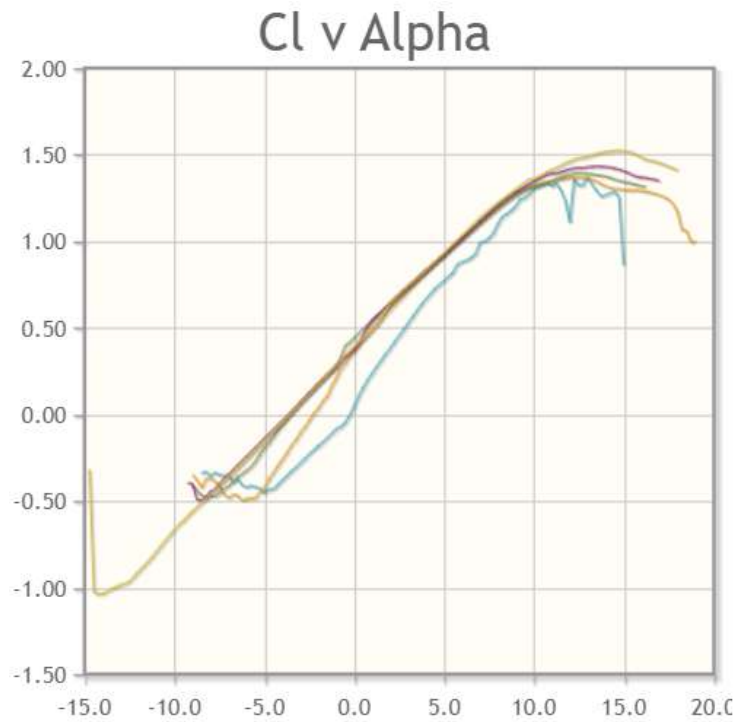


Figure 6 Airfoil Lift curve slope.

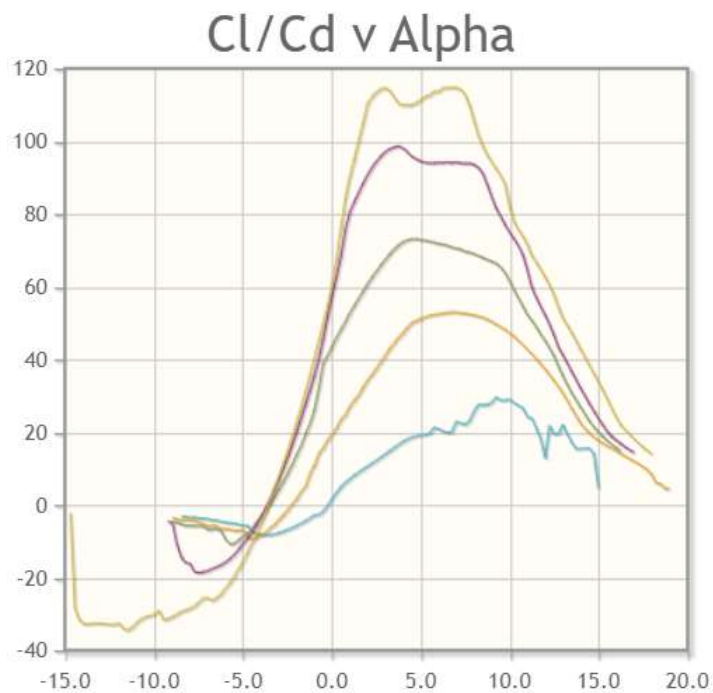


Figure 7 Aerodynamics Efficiency versus Angle of attack.

Similarly, examining the drag coefficient (C_d) versus angle of attack (α) graph provides insights into the airfoil's drag characteristics. The Clark-Y airfoil typically exhibits relatively low drag coefficients across a range of angles of attack, contributing to efficient flight

performance and allowing for higher speeds without excessive power requirements. This feature is particularly advantageous for RC aircraft where maximizing flight duration and endurance is desirable.

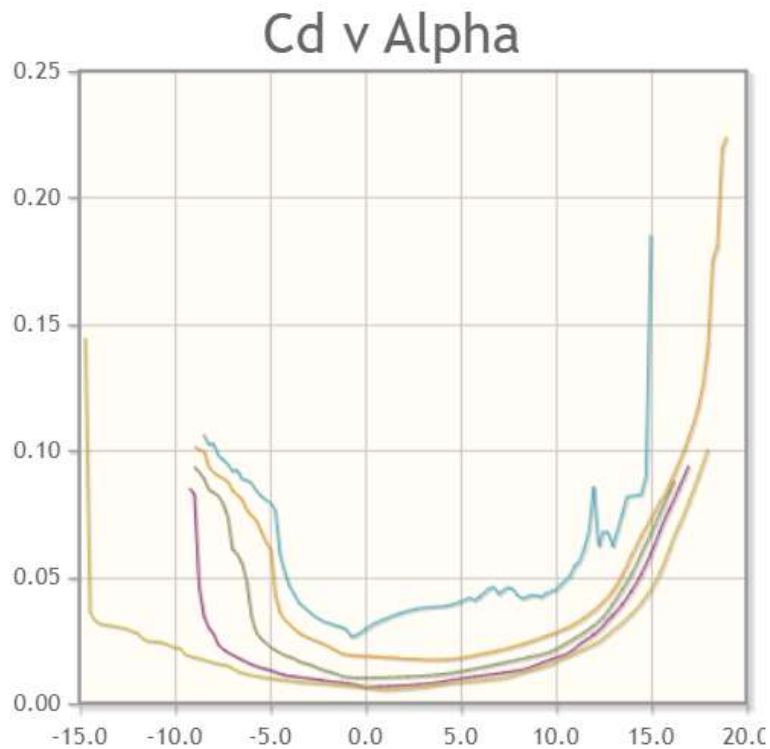


Figure 8 Drag Coefficient vs Angle of Attack

In addition to lift and drag characteristics, Airfoil Tools also offers graphical representations of other aerodynamic properties such as pitching moment coefficient (C_m) and pressure distribution. These insights further inform modelers about the airfoil's stability, control, and overall aerodynamic performance, aiding in the selection and optimization process for RC aircraft design.

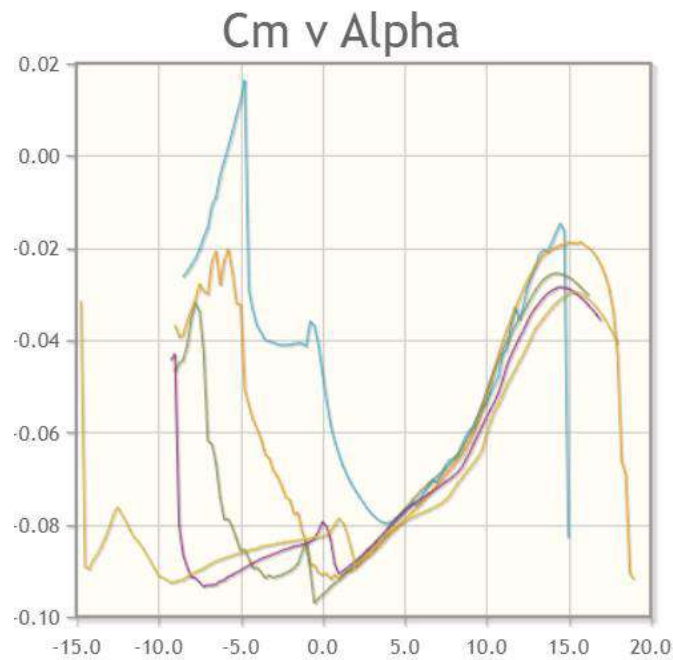


Figure 9 Pitching Moment Coefficient versus Angle of Attack

Figure 5: Basic Performance Plots of Airfoils

Based on the above data, we finalized Clark T for the following reasons:

- Better L/D ratio
- Ease of fabrication
- High stall angle of 10.7 degrees
- Maximum thickness of 11.7%

In conclusion, the Clark-Y airfoil, analyzed using tools like Airfoil Tools, offers a balanced combination of lift, drag, and stability characteristics suitable for a wide range of RC aircraft applications. By leveraging graphical representations of lift and drag coefficients, modelers can make informed decisions during the airfoil selection process, ultimately leading to optimized performance and flight characteristics for their RC aircraft designs.

Sizing Calculations and Analysis:

In order to conduct the sizing calculations as well as the analytical analysis of the aircraft, a Python code was used. The code is attached in the Appendix. The calculations performed in the code are briefly depicted in the following sections sizing, stability analysis, and performance analysis.

Wing Geometry parameters:

The following parameters were selected for the wing geometry:

Table 6 Wing Geometry Parameters

Aspect Ratio	4.66
Dihedral	0
Taper Ratio	1
Leading Edge Sweep	0

Quarter Chord Sweep	0
---------------------	---

Horizontal Tail Geometry parameters:

The following parameters were selected for the horizontal tail geometry:

Table 3: Horizontal Tail Geometry Parameters

Table 7 HT Geometry Parameters

Aspect Ratio	3.33
Dihedral	0
Taper Ratio	0.5
Leading Edge Sweep	22 degrees

Vertical Tail geometry parameters:

The following parameters were selected for the Vertical Tail geometry:

Table 4: Vertical Tail Geometry Parameters

Table 8 VT Geometry Parameters

Aspect Ratio	1.36
Taper Ratio	0.65
Leading Edge Sweep	18°

Final Design Parameters

Table 9 Final Design Parameters

Specifications	Parameters	Specifications	Parameters
Airfoil	Clark-Y	Launch Speed	Gravity Drop
Chord Length	8.75 inches	Launch Height	>100 m
Cl max	1.43	Reynold Number	210466
Cl Design	0.42	Cruise Speed	28 m/s
Wingspan	60.3 inches	Stall Speed	15 m/s
Fuselage Length		Maximum Speed	56 m/s
HT Span	20 inches	MTOW	1650
HT Chord	8.75	Empty Weight	0.8
VT Span	9.02	Wing Opening (s)	0.6 sec
VT Chord	8.03	Payload	0.3

Propulsion System

When selecting a motor for a small RC aircraft, utilizing tools like the Ecalc website can provide valuable insights into matching the motor and propeller combination for optimal performance. With a motor selected with a rating of 2300 rpm/V and a propeller size of 5x4, Ecalc allows for precise calculations of key parameters such as thrust, current draw, and efficiency. The motor's rpm/V rating indicates its rotational speed per volt applied, while the

propeller size defines its diameter and pitch. By inputting these parameters into Ecalc, modelers can simulate the performance of the motor and propeller combination, ensuring that the system generates sufficient thrust for desired flight characteristics while operating within safe current and temperature limits. This careful selection process helps to achieve a balance between power output, efficiency, and battery life, resulting in an optimized setup for small RC aircraft that meets performance requirements and enhances the overall flying experience.

setupFinder - Quick Drive Finder **@Calc**
Demo-Version - Sign-up now...
Language: english

Airplane
Wing Type: Monoplane
All-Up-Weight: 240 g / 8.5 oz
Wingspan: 368.3 mm / 14.5 inch
Wing Area: 13.1 dm² / 203 in²
Lift Coefficient (Cl): 1 (Vs. 20km/h - 13mph)
Cooling: good

desired Performance
Flight Mission: 3D - mild
Speed: 80 km/h / 49.7 mph (51km/h - 32mph)
Thrust: 150 g / 5.3 oz (432g - 15.2oz)
Flight Time: 3 min

Battery Cell
Configuration: 2 S
Voltage: LiPo - 3.7V

General
Air Temperature: 25 °C / 77 °F
Field Elevation: 500 m.ASL / 1640 ft.ASL

Motor
of Motors: 1
Gear Ratio: 1 : 1
max. Weight: 30 g (72g - 2.6oz)

Propeller
max. Diameter: 5 inch (2.3...5.8inch)
Pitch: 4.0 inch (2...4inch)
Blades: 2

Figure 10: Settings for Daughter plane.

Table sortable by clicking the header - Click a row to open in propCalc

Propeller	Motor	KV	ESC	Battery	Current	Speed		Thrust		Drive Weight	
						rpm/V	A+	Ah	OC (2s1p)	A	km/h
4.5x...	FHEM C20...	..0	5	...0mAh - ..0C (2s1p)	..3	81	50	165	5.8	38	1 ▲
4.5x...	FHEM C20...	..0	5	...0mAh - ..0C (2s1p)	..3	84	52	169	6.0	38	1
4.5x...	Surpass X18...	..0	5	...0mAh - ..0C (2s1p)	..3	72	45	150	5.3	38	1
4.5x...	Surpass X18...	..0	5	...0mAh - ..0C (2s1p)	..3	77	48	159	5.6	38	1
4.5x...	Surpass X18...	..0	5	...0mAh - ..0C (2s1p)	..3	80	50	166	5.9	38	1
4.5x...	Surpass X18...	..0	5	...0mAh - ..0C (2s1p)	..3	82	51	169	6.0	38	1
5x...	iPower IBM...	..0	10	...0mAh - ..5C (2s1p)	..4	73	45	196	6.9	39	1
5x4.0	iPower iBM2211X-2300	2300	10	200mAh - 25C (2s1p)	4	76	47	202	7.1	39	1
5x...	iPower IBM...	..0	10	...0mAh - ..5C (2s1p)	..5	78	48	206	7.3	39	1
5x...	iPower IBM...	..0	10	...0mAh - ..5C (2s1p)	..5	80	50	211	7.4	39	1
5x3.8	Maytech MTO1806-2300-MK	2300	5	200mAh - 20C (2s1p)	4	71	44	189	6.7	39	1
5x...	Avionic PRO...	..0	5	...0mAh - ..0C (2s1p)	..4	70	43	171	6.0	39	1
5x4.1	Avionic PRO M2222 KV2280	2280	5	200mAh - 20C (2s1p)	4	71	44	173	6.1	39	1
5x...	Avionic PRO...	..0	5	...0mAh - ..0C (2s1p)	..4	73	45	177	6.2	39	1
5x...	BrotherHobby VY1...	..0	10	...0mAh - ..5C (2s1p)	..5	74	46	202	7.1	39	1
5x...	BrotherHobby VY1...	..0	10	...0mAh - ..5C (2s1p)	..5	77	48	208	7.3	39	1
5x...	HGLRC Aero...	..0	10	...0mAh - ..0C (2s1p)	..5	71	44	187	6.6	39	1 ▼

Record ID: 913 248-204 of 3,505

Figure 11: Motor selection for Daughter plane.

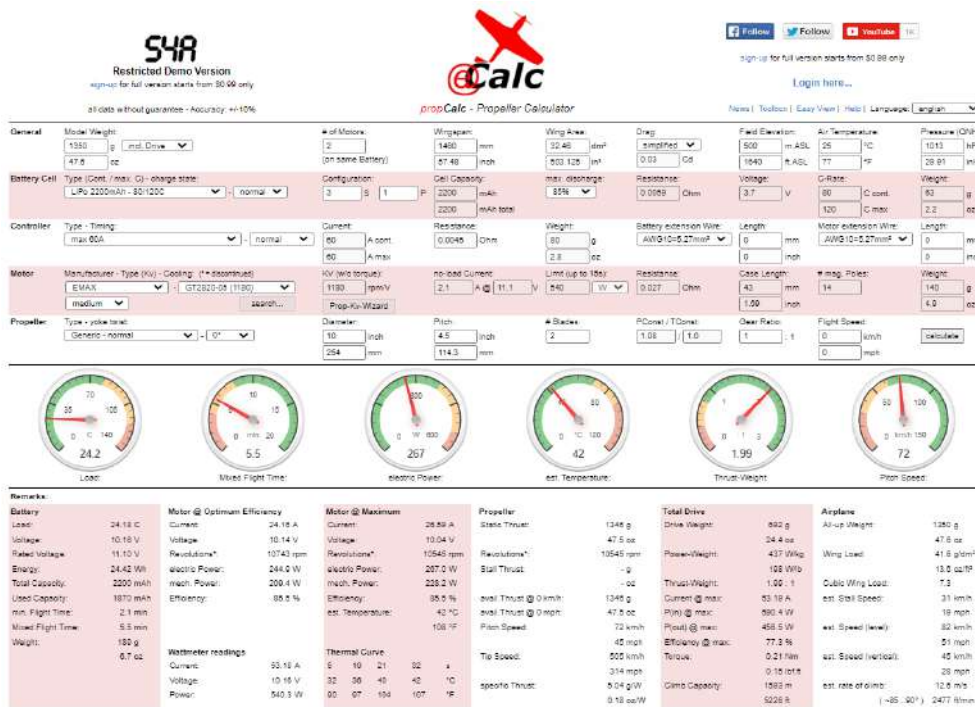


Figure 12: Without Daughter plane.

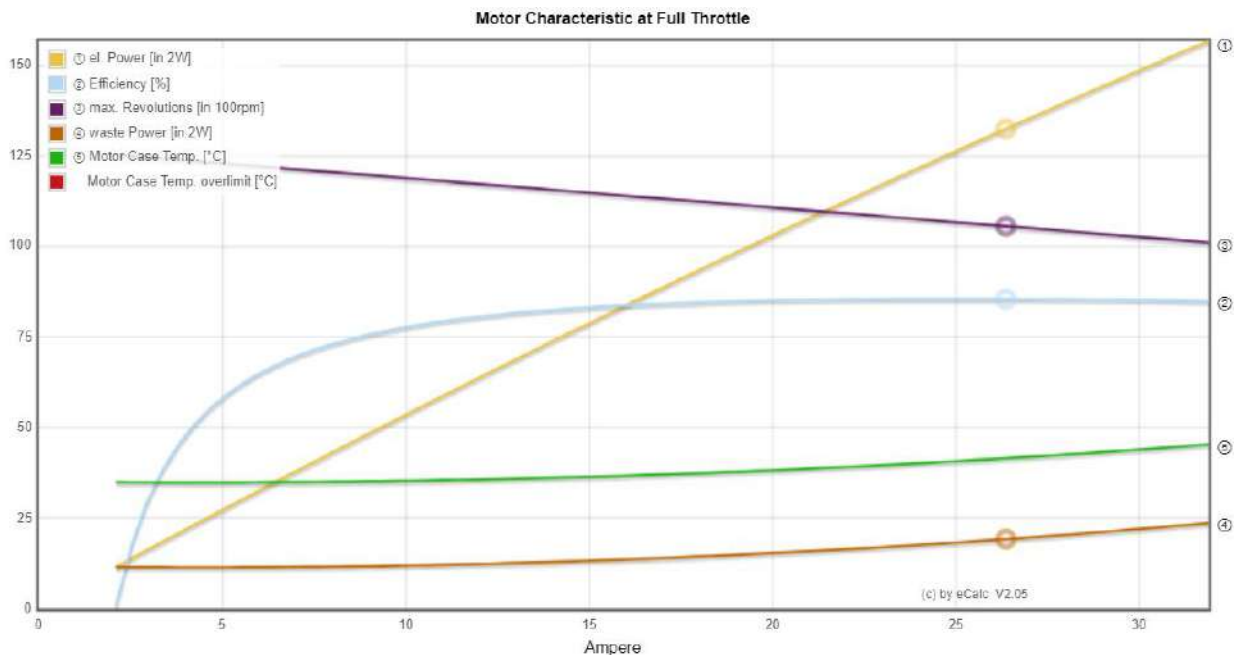


Figure 13: Performance without Daughter plane.

To simulate our model using the Ecalc software, we input the specific details of our motor, propeller, battery, and aircraft geometry to accurately predict thrust-to-weight (T/W) ratio and mixed flight time. Beginning with the motor, we provide its specifications, such as the rated RPM/V (2300 rpm/V), maximum current, and voltage. Next, we input details about the propeller, including its size (5x4), material, pitch, diameter, and blade count. For the battery configuration, we specify the type, capacity, voltage, and discharge rate, crucial for determining power supply and flight endurance. Then, we define the aircraft's geometry, such

as its weight, dimensions, wing area, fuselage length, and any other structural components. By setting flight parameters like target T/W ratio and flight profile (e.g., hovering or cruising), along with specifying the mixed flight time requirements, we ensure accurate simulations. Running the simulation in Ecalc provides us with valuable insights into expected T/W ratio and estimated mixed flight time under various conditions. We meticulously analyze these results, optimizing the setup if needed to meet performance goals. Ultimately, we validate the simulation through real-world testing, confirming its accuracy and making further adjustments as necessary, ensuring our small RC aircraft model achieves optimal performance and flight characteristics.

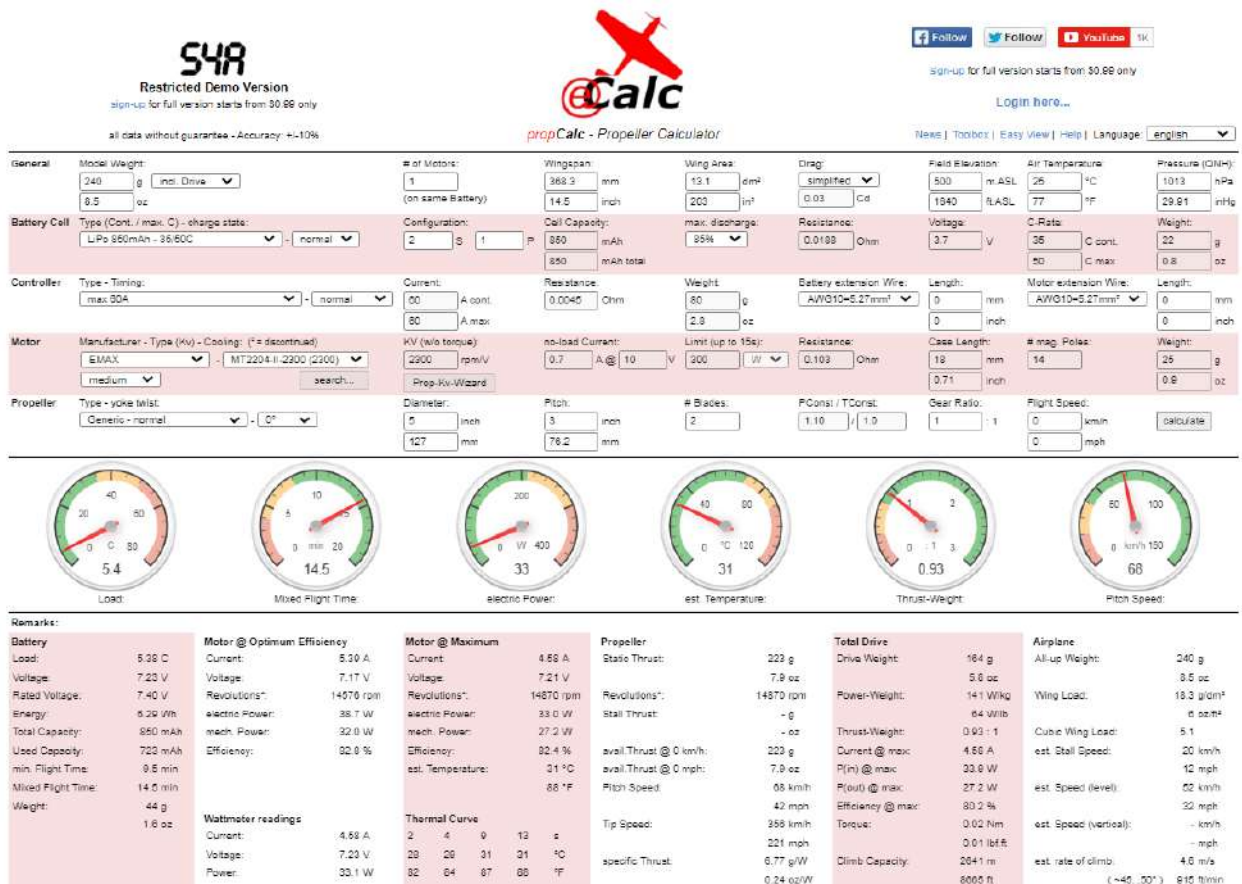


Figure 14: Daughter Plane Propulsion.

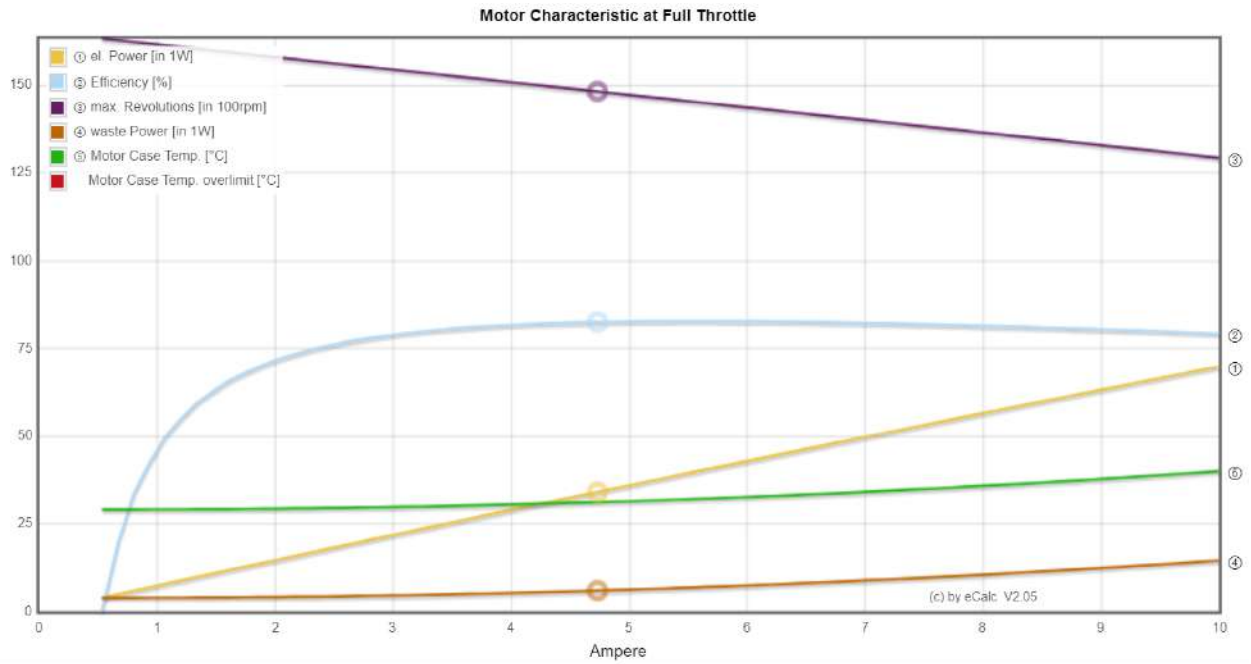


Figure 15: Daughter Plane Performance.

In simulating our parent cargo plane model using the Ecalc software, we carefully input the specifications tailored to its larger size and cargo-carrying capacity. The chosen motor features a lower RPM/V rating of 1250 rpm/V, suitable for providing ample torque and thrust required for lifting heavier payloads. Coupled with a larger propeller size of 10x4.5, this configuration ensures efficient power delivery and sufficient lift generation for cargo operations. Additionally, we select a 3S 2200mAh battery pack to supply the necessary power, balancing weight and capacity considerations for extended flight durations. Inputting the aircraft's geometry, including its weight, wingspan, fuselage dimensions, and cargo bay specifications, allows for accurate simulations tailored to its cargo-carrying capabilities. By setting flight parameters such as the desired T/W ratio and mixed flight time requirements, we anticipate the model's performance under various operating conditions. Running the simulation in Ecalc provides comprehensive insights into the expected T/W ratio and mixed flight time, enabling us to fine-tune the setup to meet cargo plane requirements effectively. Subsequent analysis and validation through real-world testing ensure that our cargo plane model achieves optimal performance, payload capacity, and flight endurance for efficient cargo transportation operations.

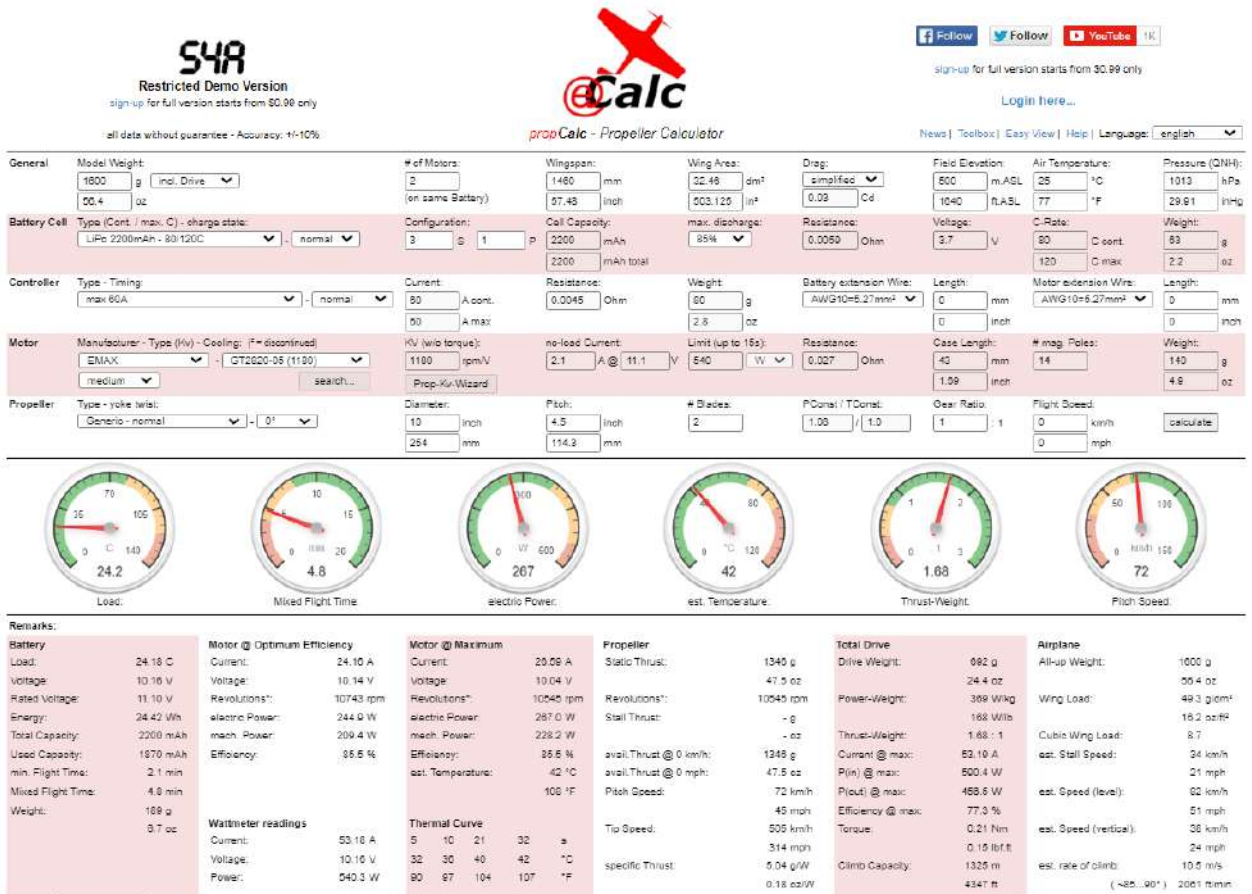


Figure 16: With Daughter plane motor calculation.

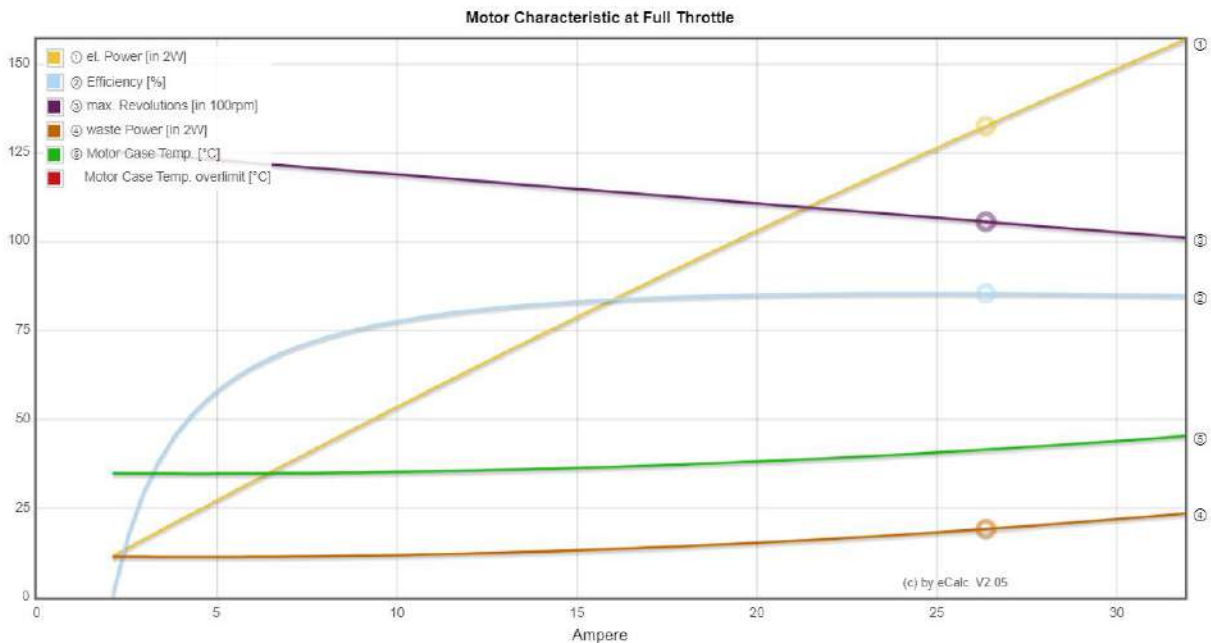


Figure 17: With daughter performance.



Figure 18 Motor Selected: GT-2820-05

Stability Analysis

Static Stability Analysis using XFLR:

Aircraft Geometry:

Description: Begin by creating or importing the 2D or 3D geometry of your aircraft into XFLR.

Explanation: Define the wing, tail surfaces, fuselage, and other components. Ensure that the geometry is accurately represented.

Define Aircraft Configuration:

Description: Set up the essential parameters that define the aircraft's configuration.

Explanation: Specify details such as wing area, aspect ratio, sweep, dihedral, control surface deflections, and other relevant characteristics. This information is crucial for static stability analysis.

Trim Aircraft for Steady-State Flight:

Description: Use the trim tool in XFLR to find the equilibrium state of the aircraft.

Explanation: Adjust control surfaces (elevator, aileron, rudder) until the aircraft achieves a state of steady, unaccelerated flight. This represents a trimmed condition, with zero net forces and moments.

Perform Static Stability Analysis:

Description: Access the static stability analysis tool within XFLR.

Explanation: Select the type of analysis you want to perform, such as Pitching Moment vs. Angle of Attack or Lift Curve Slope vs. Angle of Attack. XFLR will generate plots showing the variation of aerodynamic coefficients with changes in aircraft attitude.

Review Static Stability Results:

Description: Analyze the output from the static stability analysis.

Explanation: Evaluate static stability derivatives, including parameters like pitch moment coefficient ($C_{m\alpha}$), lift curve slope ($CL\alpha$), and others. These provide crucial insights into the aircraft's stability characteristics.

Dynamic Stability Analysis using XFLR:

Define Aircraft Configuration:

Description: Ensure the aircraft configuration is correctly set up with accurate geometric and aerodynamic parameters.

Explanation: Verify that all relevant parameters, such as mass, moments of inertia, wing loading, and control surface effectiveness, are properly defined.

Create a Flight Dynamics Model:

Description: Access the dynamic stability modeling tool in XFLR.

Explanation: Define the aircraft's dynamic characteristics, including mass properties, inertia tensors, and stability derivatives. This forms the basis for the dynamic stability analysis.

Perform Time-Domain Simulation:

Description: Specify initial conditions and run a time-domain simulation.

Explanation: Define initial values for key parameters (e.g., velocity, altitude, pitch angle). Execute the simulation to observe how the aircraft responds to perturbations and disturbances.

Analyze Dynamic Response:

Description: Examine the time-domain simulation results.

Explanation: Study time histories of crucial variables such as pitch angle, pitch rate, altitude, and control surface deflections. This provides insights into the aircraft's dynamic stability behavior.

Optional: Eigenvalue Analysis for Modes of Motion:

Description: Perform eigenvalue analysis to examine the stability modes of the aircraft.

Explanation: This analysis computes the eigenvalues of the state-space matrices, revealing information about the aircraft's modes of motion and stability characteristics.

Additional Tips:

Iterate and Validate: Conduct multiple iterations of the analysis, adjusting parameters as needed to achieve stable and realistic results. Compare the XFLR results with theoretical or experimental data if available.

Sensitivity Analysis: Explore how changes in parameters like control surface deflections, wing loading, or other design features affect static and dynamic stability.

Documentation: Keep detailed records of your configurations, settings, and results for future reference and validation.

CG Estimation

Estimating the Center of Gravity (CG) using geometry in Ecalc software involves inputting detailed specifications of the aircraft's physical dimensions and component locations to determine the optimal balance point. Beginning with the aircraft's geometry, we provide measurements such as the wingspan, fuselage length, tail length, and horizontal and vertical stabilizer dimensions. Additionally, we input the positions of key components such as the motor, battery, receiver, and any other payloads. Ecalc then utilizes this information to calculate the CG position relative to the aircraft's reference point, typically measured as a percentage of the wing's chord length from the leading edge. By accurately inputting the aircraft's geometry and component positions, Ecalc generates a CG estimation that ensures the model's stability

and controllability during flight. This estimation serves as a crucial guideline for positioning components and adjusting weight distribution to achieve the desired CG location, ultimately contributing to safe and stable flight operations.



cgCalc - Center of Gravity (CG) Calculator
 Restricted Demo Version - [sign-up](#) for full version or [login](#)

1'385'157 simulated Center of Gravity

The [cgCalc](#) of [eCalc.ch](#) not only calculates and evaluates the center of gravity (CG), neutral point (NP) and mean aerodynamic chord (MAC) but also visualizes your design of conventional aircraft, flying wing, delta or canard. Approximate complex wing design with 5 trapezoidal wing panels. For further instructions see below...

Never ever exceed Center of Gravity on maiden flight!
 Select always the more conservative CG of the manufacturer and cgCalc for your maiden flight and read the limitations below.

Aircraft or Project Name:

Wing:

Root Chord [R]: cm

Tip Chord [T1-T5]: - - - - cm

Sweep [S1 - S5]: - - - - cm

Panel Span [W1 - W5]: - - - - cm

Tail: (Tail Effectiveness)

Root Chord [R]: cm

Tip Chord [T1-T5]: - - - - cm

Sweep [S1 - S5]: - - - - cm

Panel Span [W1 - W5]: - - - - cm

Distance LE Wing to Tail [D]: cm (use negative value for canard)

AC Position: % of MAC (default: 25%)

Static Margin: % of MAC (recommended: 12.5...5%)

Fuselage:

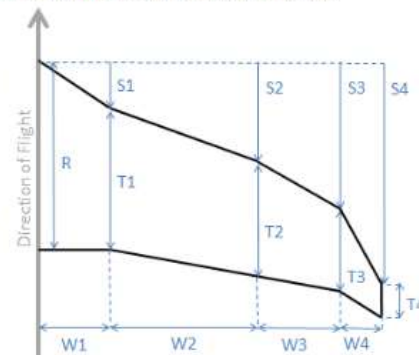
Width: cm

Length: cm

Nose Overhang: cm

Units: [Deutsch](#) | [Login](#)

Datum is the leading edge of the center chord R



(if less than 5 half wing panels are required, define the panel Chord, Sweep and span as 0 starting from the far right with W5)

Results:	Link to recall SBach 342 (Example)		
Aircraft CG range [•]:	?.28 ... ?.39 cm (@ 23.77 ... 28.77% of MAC)	Aircraft NP [•]:	?.17 cm (@ 41.27% of MAC)
Wing AC [•]:	?.56 cm (@ 25% of MAC)	Tail AC [•]:	7.39 cm (@ 25% of MAC)
Wing MAC @ Distance:	27.23 cm @ 36.51 cm	Tail MAC @ Distance:	19.96 cm @ 12.20 cm
Wing Sweep @ MAC:	0.00 cm	Tail Sweep @ MAC:	2.40 cm
Wing Span:	146.05 cm	Tail Span:	50.80 cm
Wing Area:	3245.96 cm ²	Tail Area:	1009.02 cm ²
Wing Aspect Ratio:	6.57	Tail Aspect Ratio:	2.56
Fuselage influence:	-1.23cm (= -5.55% of MAC)	Stabilizer Volume (V _{stab}):	0.74

Figure 19: Set up for CG calculation.

After CG estimation using Ecalc software, visualizing the CG position provides invaluable insight into the aircraft's stability and handling characteristics. Ecalc generates a graphical representation of the estimated CG location relative to the aircraft's geometry, typically depicted as a marker along the wing's chord line. This visualization allows modelers to precisely determine the CG's position in relation to key reference points on the aircraft, ensuring optimal weight distribution for balanced flight. By observing the CG marker within the graphical interface, modelers can assess whether the CG falls within the recommended range for safe and stable flight, adjusting component positions as necessary to achieve the desired balance. This visual representation serves as a vital tool for fine-tuning the aircraft's

configuration, enabling modelers to optimize CG placement for optimal performance and flight characteristics. Ultimately, CG visualization facilitates informed decision-making during the design and setup process, contributing to the overall success of the RC aircraft model.

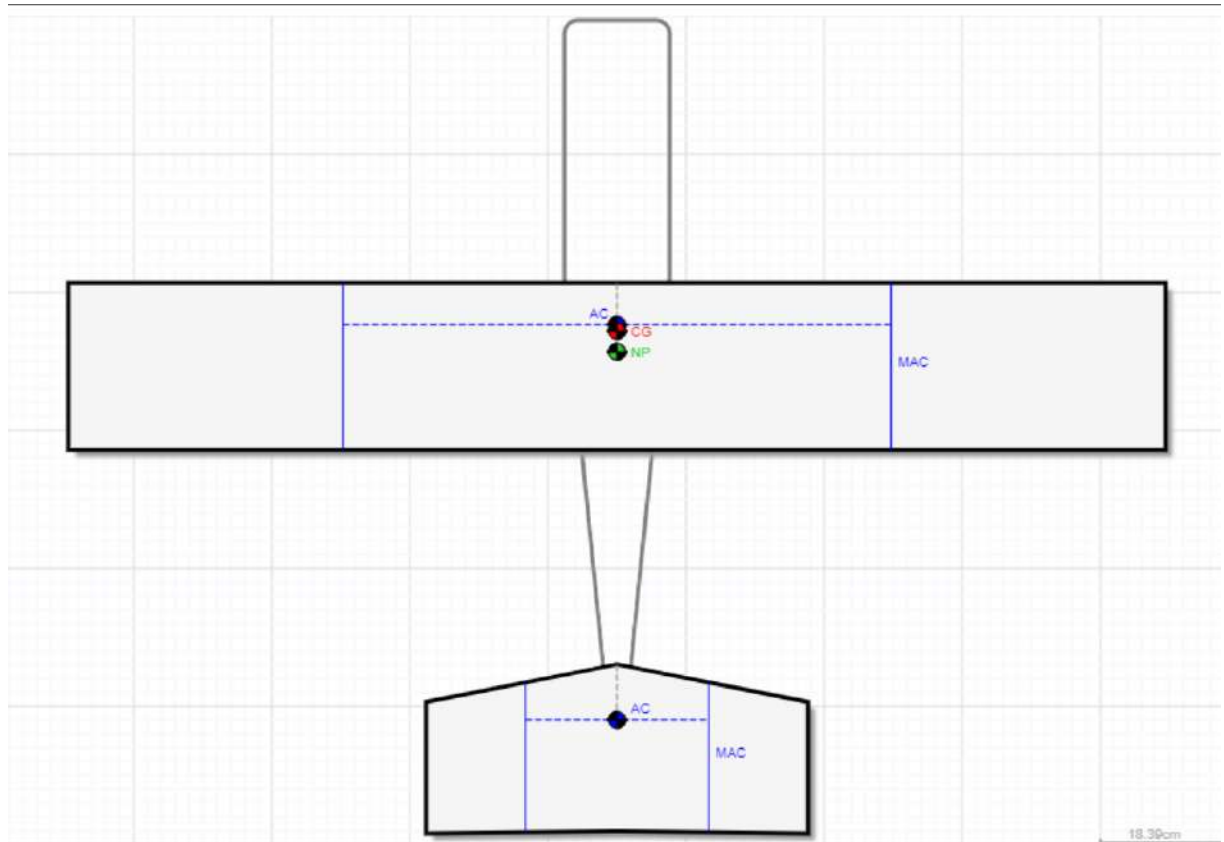


Figure 20: CG visualization in Parent plane.

In a parent cargo plane, the Center of Gravity (CG) plays a critical role in maintaining stability and flight control, especially during payload release scenarios. Before releasing the daughter small plane, the cargo plane's CG is carefully positioned to ensure balanced flight characteristics and safe handling. However, upon releasing the daughter small plane from the cargo bay, there is a noticeable shift in the cargo plane's CG. As the daughter plane exits the cargo bay, it effectively removes weight from the cargo plane, altering its overall weight distribution and CG position. This sudden reduction in payload weight can cause the cargo plane's CG to shift forward, potentially impacting its stability and controllability. Pilots must anticipate and compensate for this CG shift by adjusting control inputs to maintain stable flight conditions. Additionally, proper planning and coordination between the cargo and daughter planes are essential to mitigate any adverse effects of CG shifts and ensure the safe execution of payload release operations.

Table 10: CG Shift before and after release of Daughter plane

Neutral point	3.7 inch from leading edge of the wing
CG without Daughter aircraft	2.42 inch from the leading edge of the wing

Static Margin	1.25 inch
CG with Daughter Plane	3.1 inch from the leading edge of the wing

XFLR V5 Setup:

The XFLR model of a cargo airplane provides a comprehensive platform for aerodynamic analysis and performance prediction, essential for optimizing its design and operational parameters. Utilizing computational fluid dynamics (CFD) techniques, XFLR enables engineers and designers to simulate airflow around the cargo plane's geometry, predicting aerodynamic forces, moments, and stability characteristics with high accuracy. By inputting detailed specifications such as the aircraft's wing and fuselage geometry, airfoil profiles, and control surfaces, XFLR generates detailed aerodynamic models that facilitate a deeper understanding of the cargo plane's behavior under various flight conditions. Engineers can analyze lift, drag, and moments to optimize wing design, fuselage shaping, and control surface configurations for improved efficiency and performance. Additionally, XFLR allows for the evaluation of different payload configurations and cargo loading scenarios, enabling designers to assess the cargo plane's stability and handling characteristics under different operational conditions. Overall, the XFLR model serves as a powerful tool for enhancing the aerodynamic performance and operational capabilities of cargo airplanes, contributing to safer, more efficient, and more cost-effective transportation of goods.

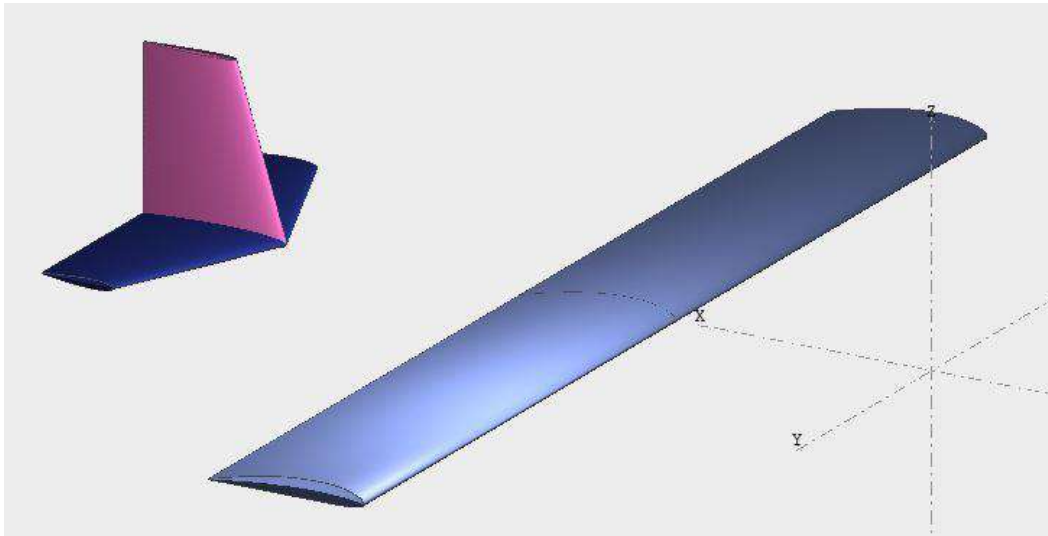


Figure 21 XFLR5 Model and Masses

Static Stability Analysis

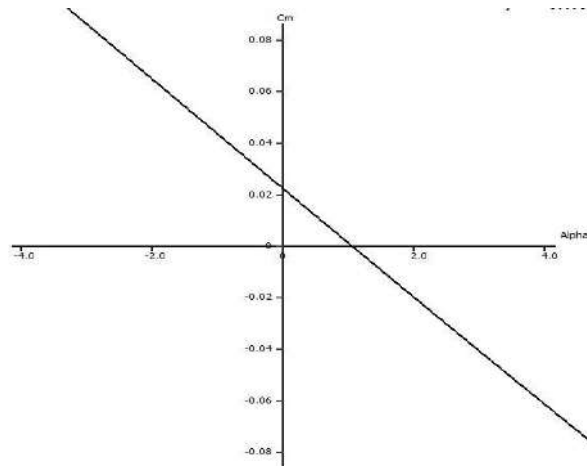


Figure 22 Pitching Moment Coefficient versus AOA Before release.

- The $C_{m\alpha}$ curve represents the relationship between the **pitching moment coefficient (C_m)** and the **angle of attack (α)** for an aircraft or airfoil.
- As the angle of attack increases (i.e., the nose of the aircraft is raised), the **pitching moment** (the tendency of the aircraft to pitch up or down) changes.
- The curve typically exhibits a **negative slope**: as α increases, C_m decreases.
- A **negative slope** indicates **stability**: when disturbed, the aircraft tends to return to its original position.

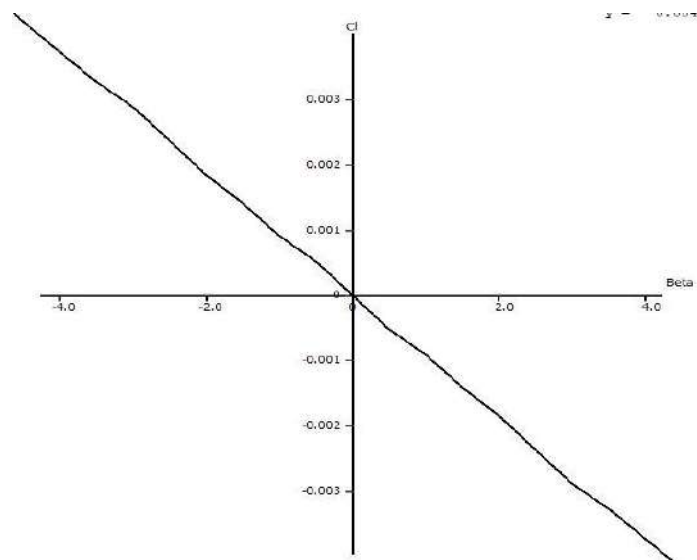


Figure 23 Rolling Moment Coefficient vs Side Slip angle.

- The **roll motion** is characterized by an absence of natural stability. There are no stability derivatives that generate moments in response to the inertial roll angle.
- When an external disturbance induces a roll, the aircraft experiences a **roll rate**. This roll rate is typically canceled out by pilot or autopilot intervention.

- The **rolling moment coefficient (Cl)** represents the effectiveness of control surfaces (such as ailerons) in generating a moment of the aircraft's center of gravity (cg) to rotate it in roll.
- The **roll axis** is usually defined as the **longitudinal axis** (from nose to tail), and the rolling moment can result from wind gusts, control surface deflections, or flying at an angle of sideslip

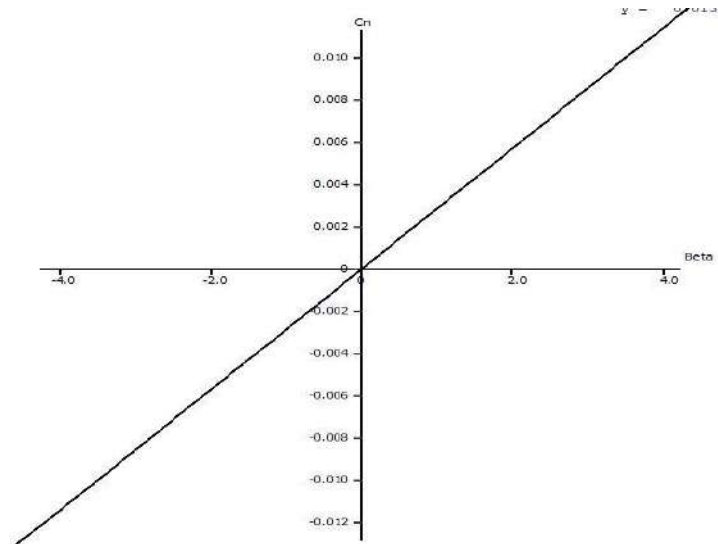


Figure 24 Yawing Moment Coefficient vs Side slip angle.

- The graph shows a straight line passing through the origin (0,0), indicating a linear relationship.
- The x-axis is labeled "Beta" (sideslip angle), ranging from -4.0 to 4.0.
- The y-axis is labeled "Cn" (yawing moment coefficient), with values ranging from -0.012 to 0.012.
- The positive slope of the line suggests that as the sideslip angle (Beta) increases, the yawing moment (Cn) also increases.

Dynamic Stability Analysis

Root Locus:

The root locus method is a powerful tool used in control theory to analyze the dynamic stability of systems, particularly in the longitudinal domain of aircraft dynamics. In this context, the longitudinal dynamics involve the pitch motion of the aircraft, which is crucial for maintaining stability and control during flight. The root locus provides insights into how the system's poles, representing the eigenvalues of the system's transfer function, change as a parameter, such as the aircraft's speed or control surface deflection, varies.

In the longitudinal domain, the root locus analysis focuses on the poles associated with the pitching motion of the aircraft, which directly influences its stability. By plotting the locus of the roots (poles) of the characteristic equation on the complex plane as the parameter varies, engineers can visualize how changes in system parameters affect the stability of the aircraft.

The root locus diagram illustrates regions of stability and instability, as well as the behavior of the system's response to changes in parameters. For instance, as certain parameters vary, poles may move towards or away from the imaginary axis, indicating changes in stability and dynamic response. Engineers can use this information to design control systems that ensure the aircraft remains stable under various flight conditions.

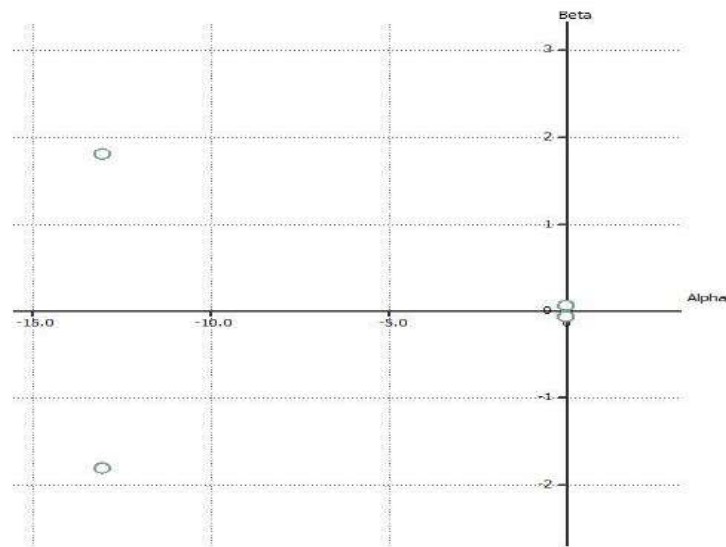


Figure 25 Longitudinal Dynamic Stability Root Locus

In the context of longitudinal stability, root locus analysis is particularly useful for designing control systems, such as elevators or stabilizers, to maintain the desired pitch attitude and stability margins. By analyzing the root locus, engineers can determine the appropriate controller gains or system parameters needed to achieve desired stability characteristics, such as damping ratio and natural frequency.

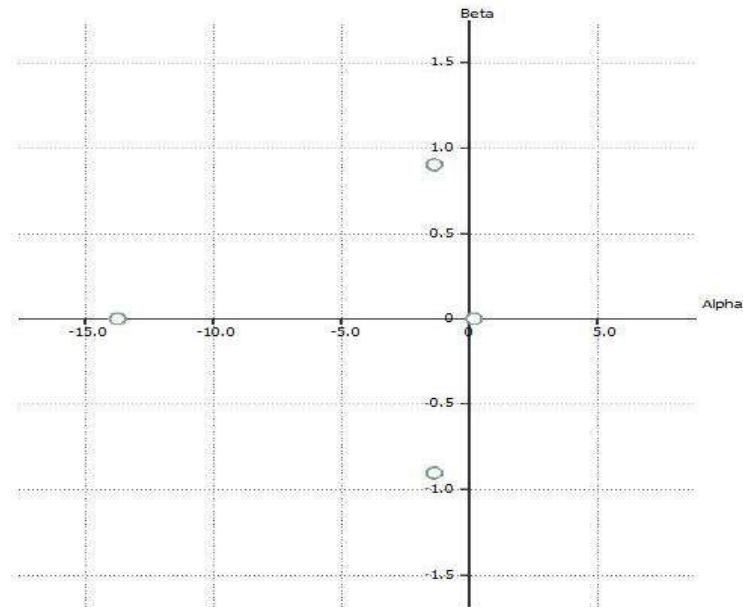


Figure 26 Lateral Dynamic Stability Root Locus

In the lateral domain of aircraft dynamics, dynamic stability is crucial for ensuring safe and controlled flight, particularly concerning the roll and yaw motions of the aircraft. The root locus method serves as a valuable tool for analyzing the lateral stability of aircraft systems. By plotting the locus of the roots (poles) of the characteristic equation on the complex plane as a parameter, such as the aircraft's speed or control surface deflection, varies, engineers gain insights into how changes in system parameters affect lateral stability. In the context of lateral stability, the root locus diagram illustrates regions of stability and instability, depicting how system poles move in response to changes in parameters. This visualization aids engineers in designing control systems, such as ailerons or rudders, to maintain desired roll and yaw attitudes and stability margins. By analyzing the root locus, engineers can determine optimal controller gains or system parameters to achieve lateral stability requirements, ensuring safe and responsive aircraft handling in various flight conditions.

Static Stability Analysis after Release

After the release of the daughter plane from the parent cargo plane, static stability analysis becomes crucial for assessing the stability of both aircraft during and after the separation event. Static stability refers to the aircraft's tendency to return to its original equilibrium position following a disturbance, such as the release of a payload. In this scenario, engineers evaluate the static stability of both the parent cargo plane and the daughter plane to ensure they can maintain stable flight conditions post-release. Factors such as the change in weight distribution, aerodynamic forces, and control surface effectiveness are considered in the analysis. By assessing the static stability of both aircraft, engineers can determine if any corrective measures, such as adjusting control inputs or flight parameters, are necessary to maintain stability and control throughout the separation event and subsequent flight phases. Additionally, static stability analysis aids in identifying potential risks or challenges associated with payload release operations, allowing for the implementation of appropriate safety measures to mitigate any adverse effects on aircraft stability and performance.

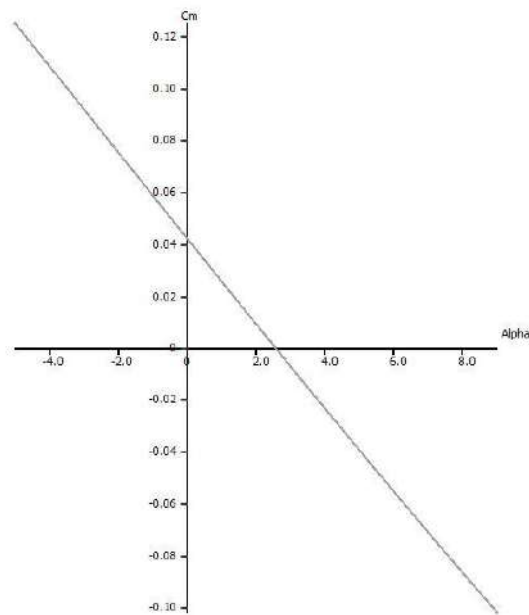


Figure 27 Pitching Moment Coefficient versus AOA after release.

The C_m curve is a fundamental representation of the relationship between the pitching moment coefficient (C_m) and the angle of attack (α) for an aircraft or airfoil. As the angle of attack increases, indicating a rise in the nose of the aircraft relative to the oncoming airflow, the pitching moment - the tendency of the aircraft to pitch up or down - undergoes changes. Typically, the C_m curve exhibits a negative slope: as α increases, C_m decreases. This negative slope is indicative of stability within the aerodynamic system. Specifically, it signifies that as the aircraft experiences a disturbance, such as a gust of wind or a maneuver initiated by the pilot, it tends to naturally return to its original position. In other words, the aircraft exhibits a self-stabilizing behavior in response to changes in angle of attack. Understanding the C_m curve is essential for aircraft designers, pilots, and engineers, as it provides critical insights into the aircraft's stability characteristics and helps in designing control systems that ensure safe and stable flight operations across a range of flight conditions.

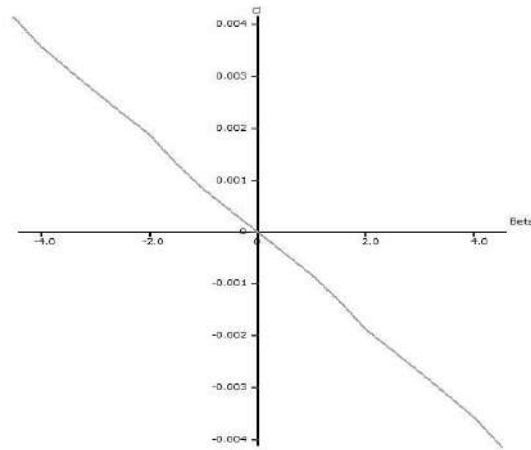


Figure 28 Rolling Moment Coefficient versus AOA after release.

The roll motion of an aircraft is characterized by an absence of inherent natural stability, meaning there are no stability derivatives that generate moments in response to the inertial roll angle. When an external disturbance induces a roll, such as a gust of wind or turbulence, the aircraft experiences a roll rate. This roll rate can be countered and controlled through pilot or autopilot intervention, where control inputs are made to stabilize the aircraft and return it to its desired attitude. The effectiveness of control surfaces, such as ailerons, in generating a moment about the aircraft's center of gravity (CG) to induce roll is represented by the rolling moment coefficient (Cl). This coefficient quantifies how effectively control inputs can rotate the aircraft about its longitudinal axis (from nose to tail) and is essential for maintaining control during maneuvers. The roll axis, typically aligned with the aircraft's longitudinal axis, can be influenced by various factors, including wind gusts, control surface deflections, or flying at an angle of sideslip. Understanding these dynamics is crucial for pilots and engineers alike, as it enables them to anticipate and counteract roll disturbances effectively, ensuring stable and controlled flight operations.

The following graph illustrates a linear relationship between the sideslip angle (Beta) and the yawing moment coefficient (Cn). It depicts a straight line passing through the origin (0,0), indicating that the relationship between Beta and Cn is linear. On the x-axis, Beta, representing the sideslip angle, ranges from -4.0 to 4.0, while the y-axis represents Cn, the yawing moment coefficient, with values ranging from -0.012 to 0.012. The positive slope of the line indicates that as the sideslip angle (Beta) increases, the yawing moment (Cn) also increases. This suggests that the aircraft experiences an increasing tendency to yaw in response to sideslip, which is a common characteristic in aerodynamic behavior. Understanding this relationship is essential for pilots and engineers, as it helps in predicting and mitigating the effects of sideslip on aircraft stability and control, particularly during crosswind conditions or other situations where sideslip angles may vary.

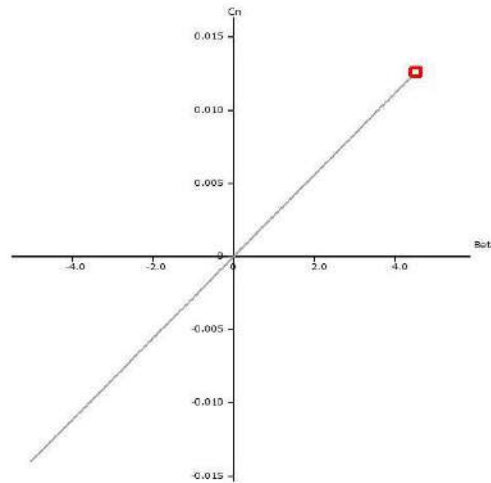


Figure 29 Yawing Moment Coefficient versus AOA after release.

The root locus method is a powerful tool used in control theory to analyze the dynamic stability of systems, particularly in the longitudinal domain of aircraft dynamics. In this context, the longitudinal dynamics involve the pitch motion of the aircraft, which is crucial for maintaining stability and control during flight. The root locus provides insights into how the system's poles, representing the eigenvalues of the system's transfer function, change as a parameter, such as the aircraft's speed or control surface deflection, varies.

In the longitudinal domain, the root locus analysis focuses on the poles associated with the pitching motion of the aircraft, which directly influences its stability. By plotting the locus of the roots (poles) of the characteristic equation on the complex plane as the parameter varies, engineers can visualize how changes in system parameters affect the stability of the aircraft.

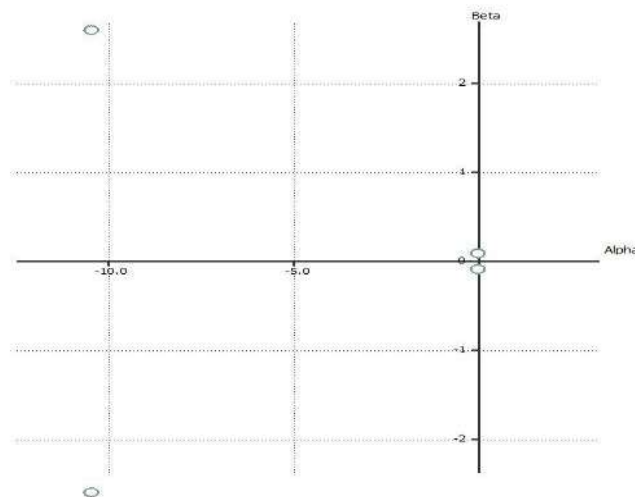


Figure 30 Longitudinal Dynamic Stability Root Locus after release.

The root locus diagram illustrates regions of stability and instability, as well as the behavior of the system's response to changes in parameters. For instance, as certain parameters vary, poles may move towards or away from the imaginary axis, indicating changes in stability and dynamic response. Engineers can use this information to design control systems that ensure the aircraft remains stable under various flight conditions.

In the context of longitudinal stability, root locus analysis is particularly useful for designing control systems, such as elevators or stabilizers, to maintain the desired pitch attitude and stability margins. By analyzing the root locus, engineers can determine the appropriate controller gains or system parameters needed to achieve desired stability characteristics, such as damping ratio and natural frequency.

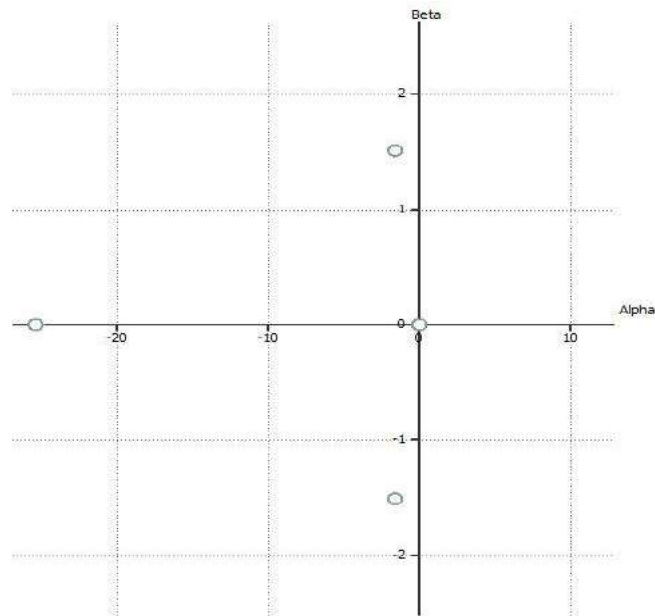


Figure 31 Lateral Dynamic Stability Root Locus after release.

In the lateral domain of aircraft dynamics, dynamic stability is crucial for ensuring safe and controlled flight, particularly concerning the roll and yaw motions of the aircraft. The root locus method serves as a valuable tool for analyzing the lateral stability of aircraft systems. By plotting the locus of the roots (poles) of the characteristic equation on the complex plane as a parameter, such as the aircraft's speed or control surface deflection, varies, engineers gain insights into how changes in system parameters affect lateral stability. In the context of lateral stability, the root locus diagram illustrates regions of stability and instability, depicting how system poles move in response to changes in parameters. This visualization aids engineers in designing control systems, such as ailerons or rudders, to maintain desired roll and yaw attitudes and stability margins. By analyzing the root locus, engineers can determine optimal controller gains or system parameters to achieve lateral stability requirements, ensuring safe and responsive aircraft handling in various flight conditions.

Modal Time Responses

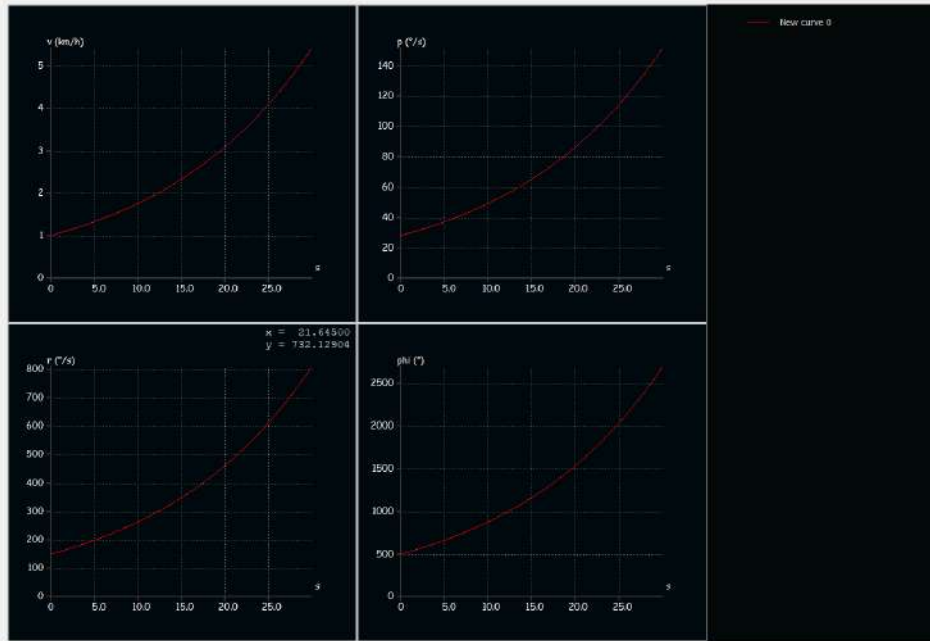


Figure 32 Directional Divergence Mode

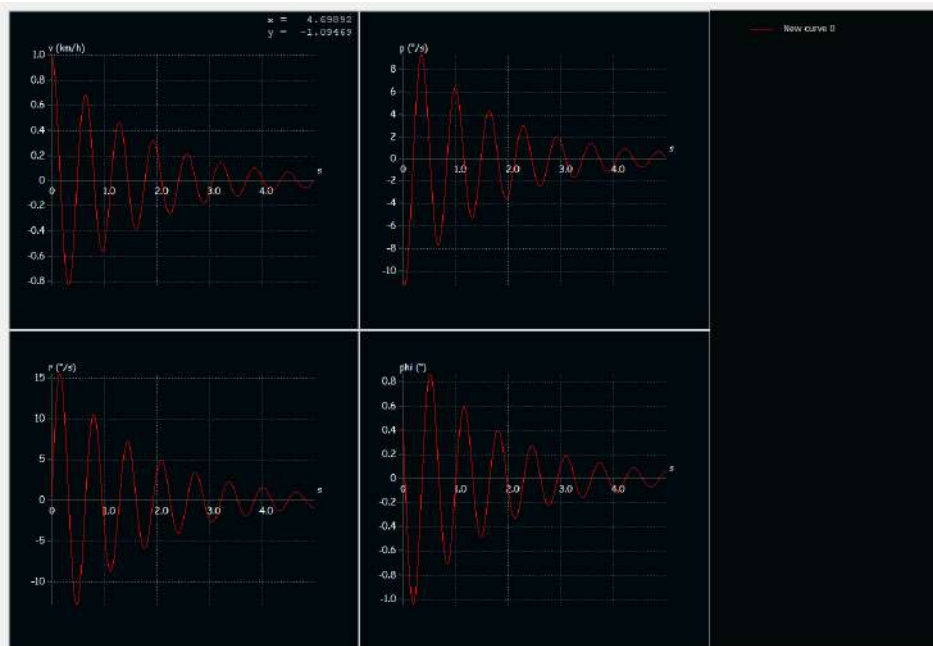


Figure 33 Dutch Roll Mode

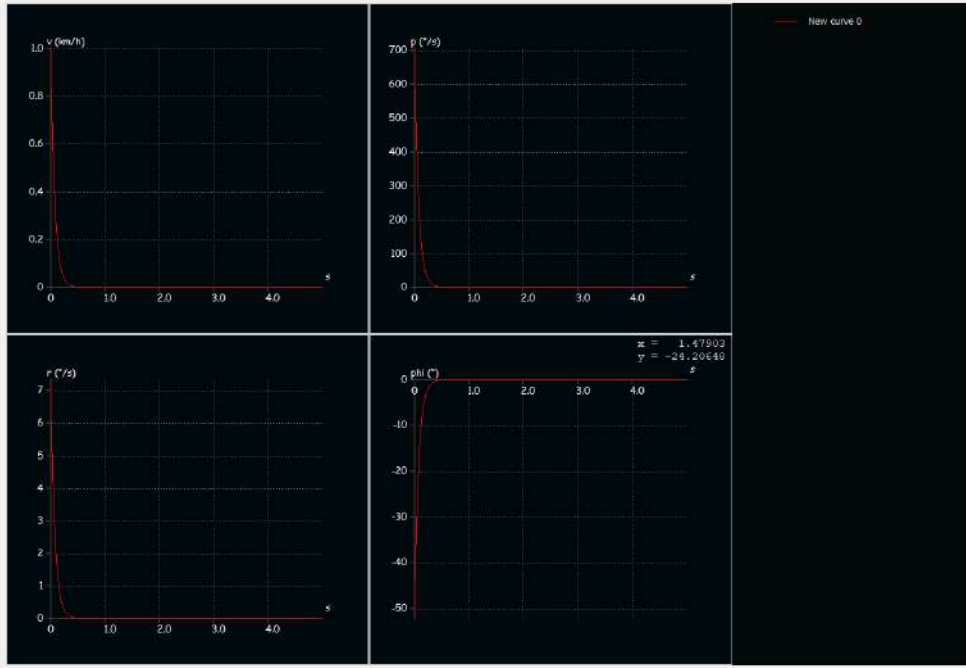


Figure 34 Roll mode.

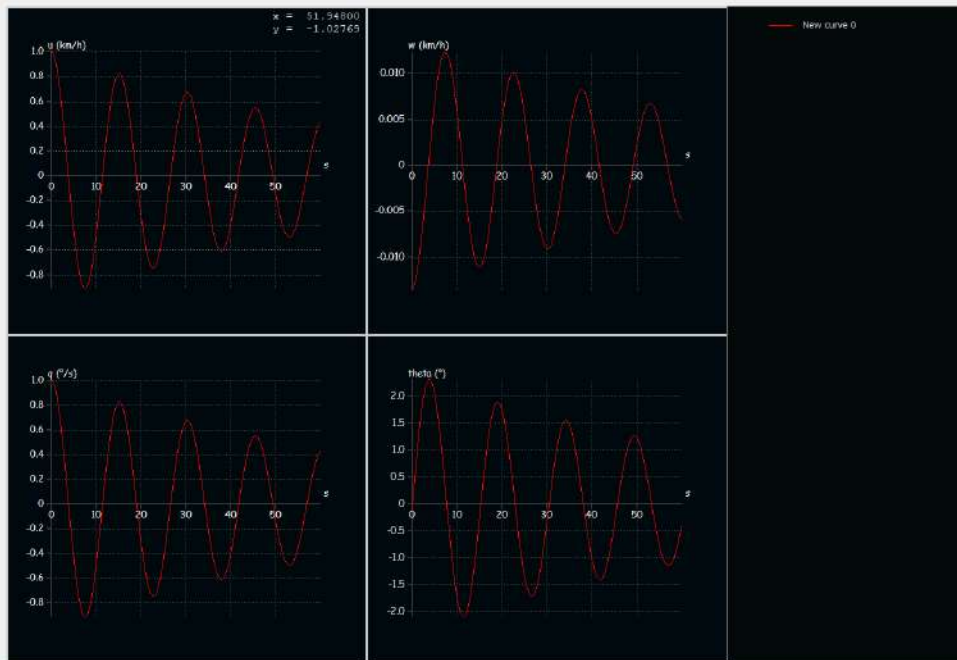


Figure 35 Long Period or Phugoid mode.

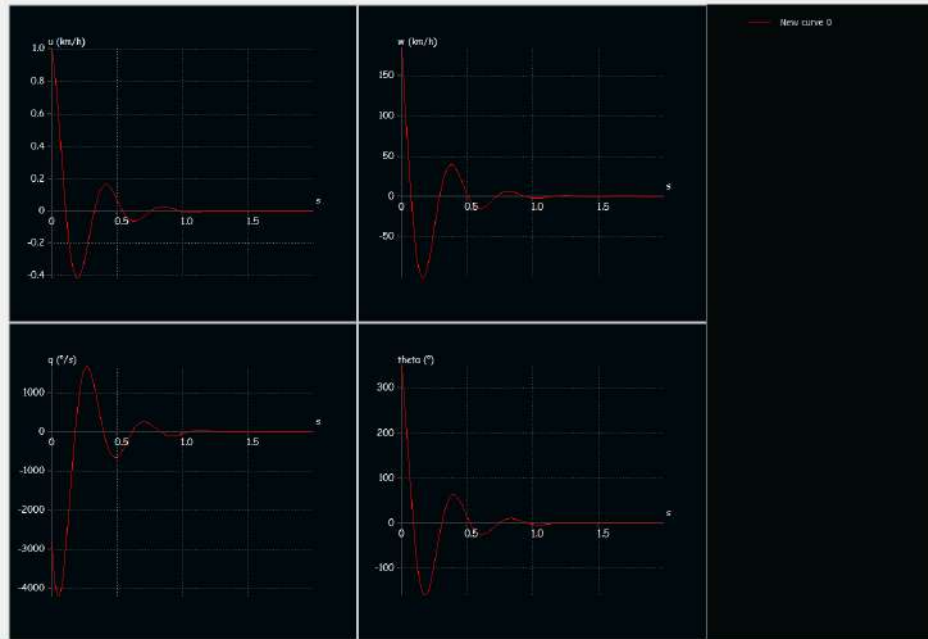


Figure 36 Short Period Mode

Performance Analysis

The plot of the coefficient of lift (CL) versus the coefficient of drag (CD) is a fundamental representation of an airfoil or aircraft's aerodynamic performance. This graph typically displays a parabolic increase of CL with CD, illustrating the trade-off between lift generation and drag production. As the angle of attack increases, leading to higher lift coefficients, the corresponding increase in drag coefficients is represented by the upward slope of the curve. This relationship signifies that as an aircraft generates more lift to sustain flight or achieve desired maneuvers, it also experiences an increase in drag, which can affect its overall efficiency and performance.

One crucial point of interest visualized on this graph is the point of drag at zero lift. This point represents the condition where the aircraft or airfoil is producing no lift ($CL = 0$) but still experiencing drag ($CD > 0$). In practical terms, this signifies the aerodynamic penalty incurred by the aircraft even when it's not actively generating lift. Factors contributing to drag at zero lift can include form drag from the airfoil's shape, skin friction drag along its surface, and interference drag from various components of the aircraft.

Understanding the implications of the drag at zero lift is vital for aircraft designers and engineers as they strive to optimize aerodynamic efficiency. Minimizing drag at zero lift is crucial for enhancing an aircraft's overall performance, especially during cruising or level flight conditions where lift production may be minimal. Design strategies such as refining airfoil shapes, reducing surface roughness, and streamlining aircraft components can help mitigate drag at zero lift, leading to improvements in fuel efficiency, range, and overall flight characteristics.

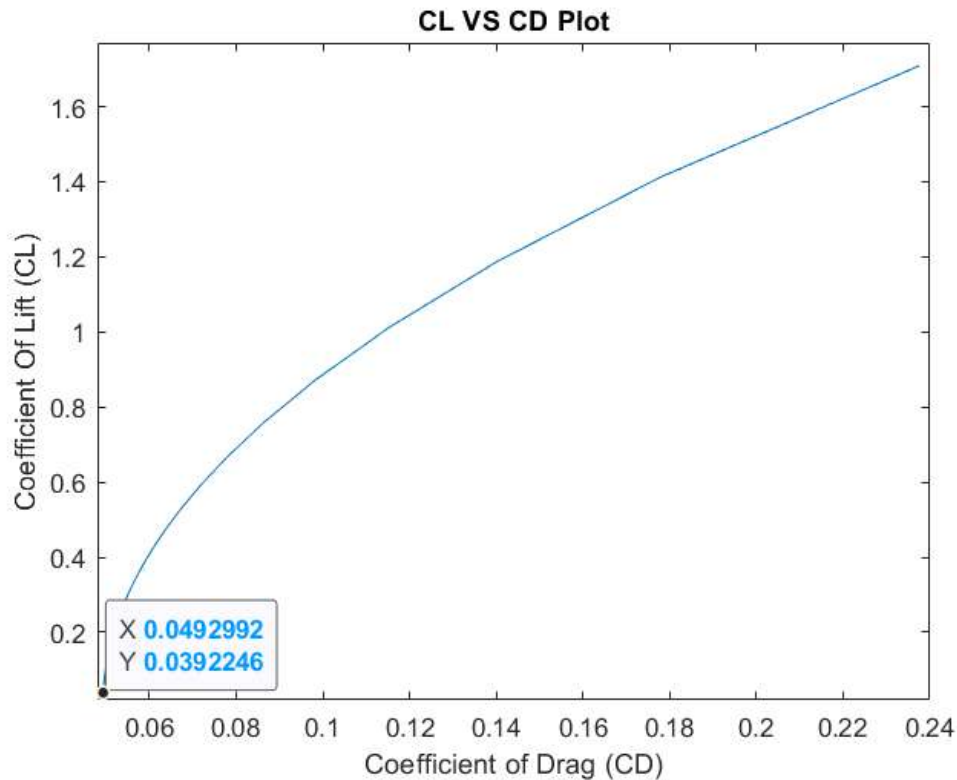


Figure 37 Aircraft Drag Polar

The graph depicting the aerodynamic efficiency curves with velocity showcases a fundamental aspect of aerodynamic performance: the relationship between velocity and efficiency. Each curve represents the aerodynamic efficiency of a particular configuration or design, and they all exhibit a common characteristic: reaching a maximum value at a certain velocity before declining.

At lower velocities, the aerodynamic efficiency typically increases as the aircraft or airfoil operates within its optimal flight regime. As velocity increases, the airflow over the airfoil or aircraft wings generates more lift relative to the drag produced, resulting in higher efficiency. This increase in efficiency continues until reaching a point where the aerodynamic forces are balanced, and the aerodynamic efficiency peaks.

After this maximum point, the efficiency begins to decrease as velocity continues to rise. This decline in efficiency can be attributed to various factors such as increased drag from higher airspeeds, changes in airflow patterns, or the onset of compressibility effects at transonic and supersonic speeds.

Understanding the behavior of aerodynamic efficiency with velocity is crucial for aircraft designers and engineers in optimizing performance across different flight regimes. By identifying the velocity at which maximum efficiency occurs, designers can tailor aircraft configurations and operating conditions to maximize performance while minimizing fuel consumption and operational costs.

Moreover, recognizing the point of diminishing returns beyond the peak efficiency velocity is essential for operational planning and decision-making. Pilots and operators must be aware of

these characteristics to optimize flight profiles, manage fuel consumption, and ensure safe and efficient operation of aircraft across various flight conditions and mission profiles.

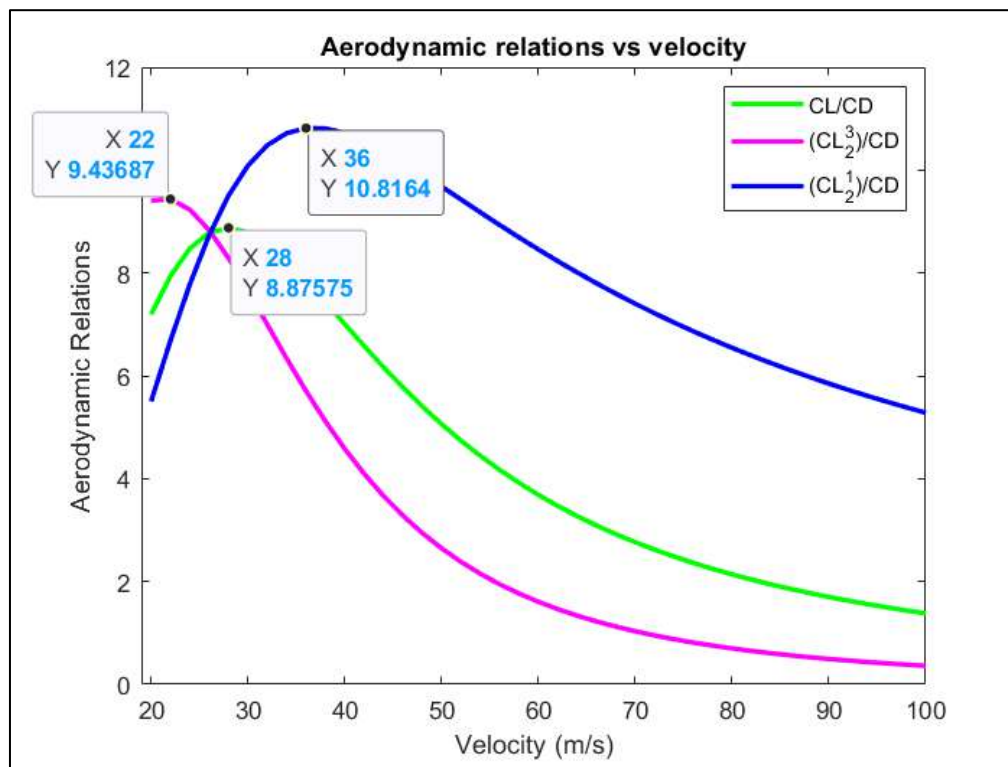


Figure 38 Important Aerodynamic Relations vs Velocity.

The thrust required graph provides a crucial insight into the relationship between velocity, drag, and the amount of thrust needed to overcome drag for sustained flight. As velocity increases, the total drag experienced by the aircraft also increases, encompassing various components such as parasite drag, induced drag, and any other forms of drag encountered during flight. The graph illustrates this phenomenon by showing a gradual rise in the thrust required as velocity increases.

This increase in thrust required is directly proportional to the velocity and drag experienced by the aircraft, as stated by the thrust equation, where thrust equals velocity multiplied by drag. As velocity rises, the aircraft encounters greater resistance from the surrounding air, resulting in higher drag forces that must be overcome to maintain forward motion. Consequently, the thrust required to counteract these drag forces also escalates proportionally.

Understanding the thrust required graph is essential for aircraft designers, pilots, and operators as it provides valuable information for flight planning, performance optimization, and aircraft operations. Pilots rely on this data to determine the power settings needed for different phases of flight, such as takeoff, climb, cruise, and descent, to ensure that the aircraft can maintain desired airspeeds and altitudes efficiently.

For aircraft designers and engineers, the thrust required graph serves as a basis for optimizing propulsion systems, airframe designs, and operational procedures to minimize drag, maximize aerodynamic efficiency, and enhance overall aircraft performance. By analyzing this graph,

designers can identify opportunities to reduce drag through aerodynamic improvements, streamline aircraft shapes, and refine engine performance to achieve optimal thrust-to-drag ratios across various flight conditions.

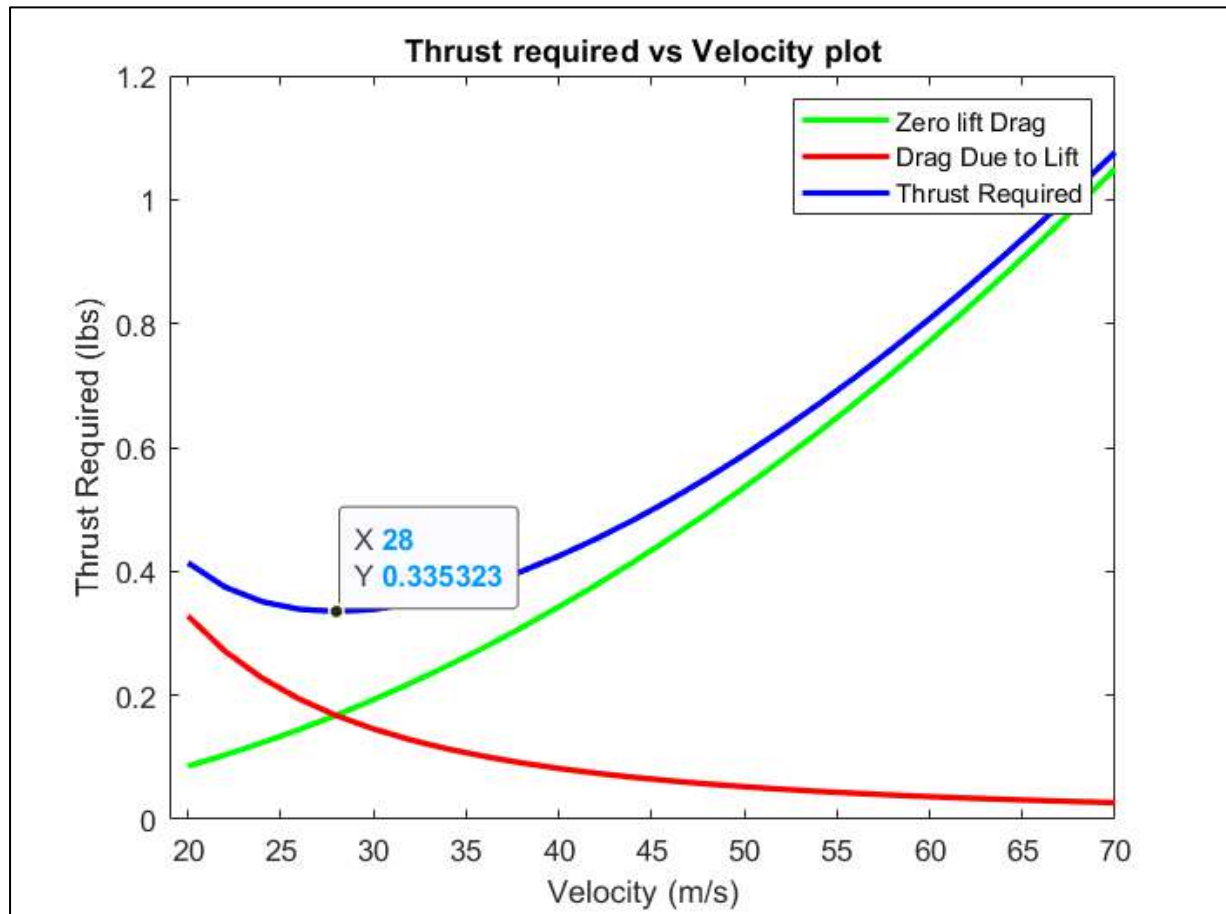


Figure 39 Thrust Required vs Velocity.

The Glide descent graph represents a fundamental aspect of aircraft performance during descent, showcasing the relationship between velocity and glide rate. As velocity increases, the graph illustrates a parabolic decrease in glide rate, highlighting the diminishing rate of descent as the aircraft accelerates. This analytical tool is invaluable for determining the required glide rate at a given velocity, offering insights into the nuanced interplay between these two parameters.

Understanding the Glide descent graph is crucial for optimizing flight dynamics and fine-tuning aircraft performance during descent phases. Pilots utilize this information to adjust their descent profiles, ensuring that they achieve the desired rate of descent while maintaining safe airspeeds and altitudes. By referencing the graph, pilots can make real-time decisions to optimize fuel efficiency, minimize descent time, and comply with air traffic control instructions.

For aircraft designers and engineers, the Glide descent graph serves as a valuable tool for optimizing aircraft configurations, flight control systems, and operational procedures. By analyzing the graph, designers can identify opportunities to enhance glide performance, such as refining wing designs, optimizing aerodynamic profiles, and implementing advanced flight

control algorithms. These optimizations ultimately contribute to improved efficiency, safety, and performance during descent operations.

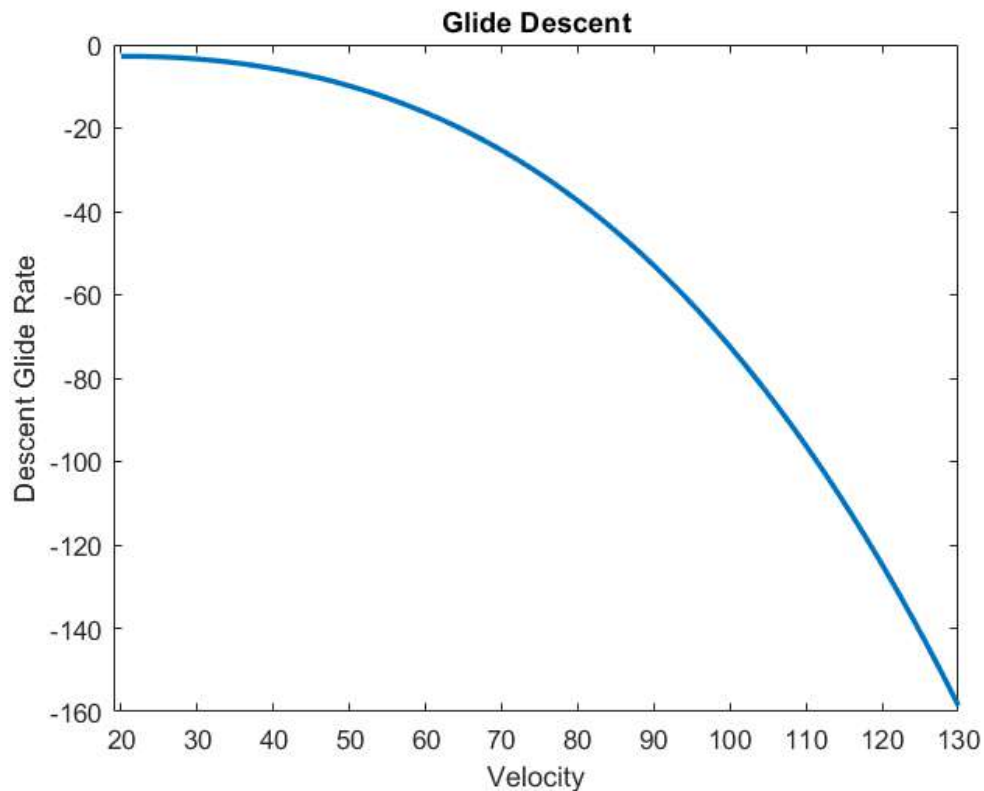


Figure 40 Sink rate vs Velocity.

The Aerodynamic Efficiency versus Velocity plot is a crucial tool for evaluating the performance of an aircraft across different flight regimes. One significant aspect of this plot is the point at which the aerodynamic efficiency reaches its maximum value. This point holds considerable importance as it indicates the velocity at which the aircraft achieves its highest efficiency, making it ideal for various flight objectives such as loitering, endurance, or maximizing range.

For instance, in applications requiring extended endurance or loitering, such as surveillance missions or aerial reconnaissance, flying at the velocity corresponding to the maximum aerodynamic efficiency ensures that the aircraft can maintain flight for an extended period while conserving fuel. Similarly, in scenarios where maximizing range is paramount, such as long-distance flights or aerial refueling operations, operating the aircraft at the velocity corresponding to peak efficiency allows for optimal fuel economy and extended flight ranges. Understanding the velocity at which the aerodynamic efficiency hits its maximum point is essential for pilots, operators, and mission planners as it informs strategic decisions regarding flight planning, fuel management, and operational tactics. By leveraging this information, pilots can optimize their flight profiles to achieve maximum efficiency and accomplish mission objectives effectively.

Moreover, for aircraft designers and engineers, identifying the velocity associated with peak aerodynamic efficiency provides valuable insights into optimizing aircraft configurations, performance characteristics, and operational capabilities. By designing aircraft to operate

efficiently at velocities corresponding to maximum efficiency, designers can enhance overall performance, fuel economy, and mission effectiveness.

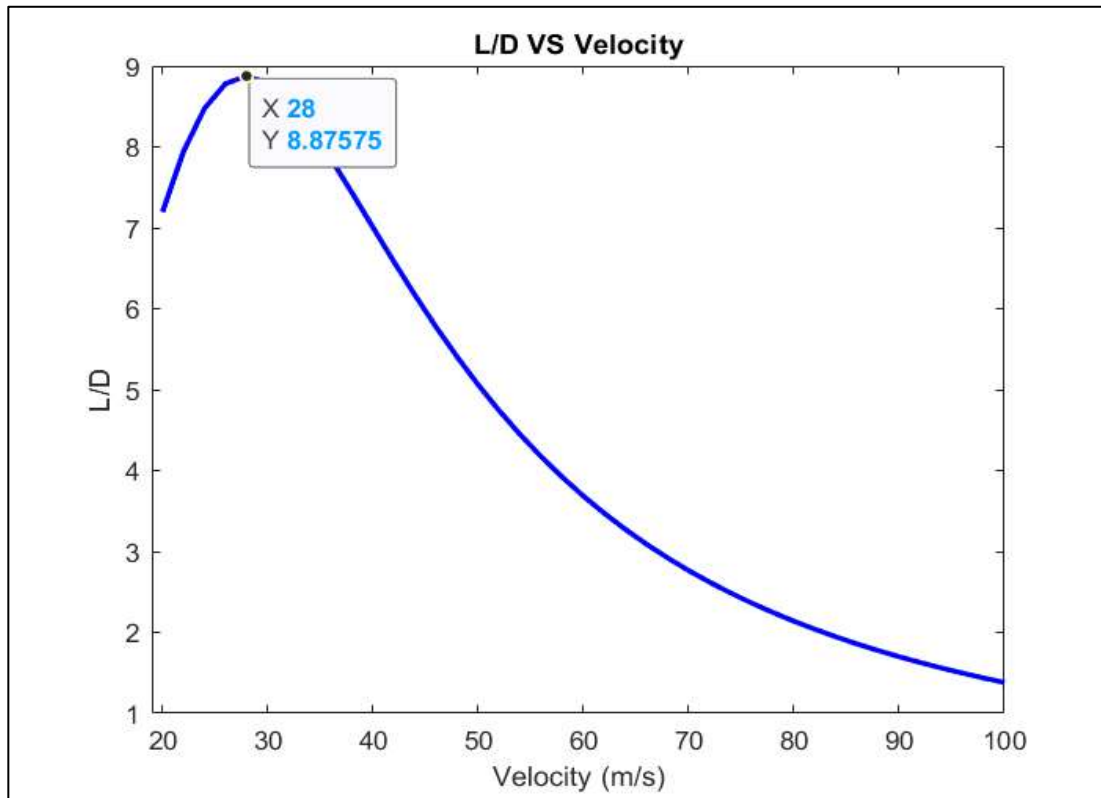


Figure 41 Aerodynamic Efficiency vs Velocity.

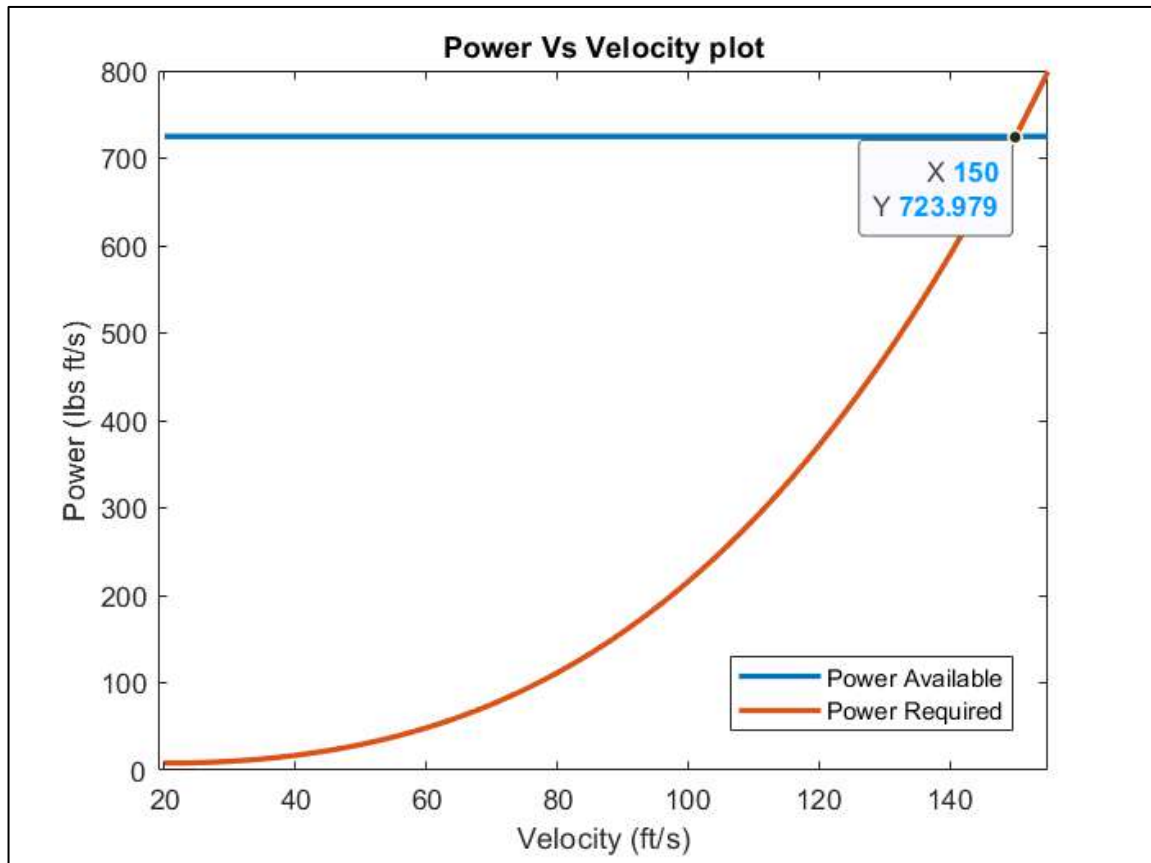


Figure 42 Power available and Power Required vs Velocity.

The combined plot of Power Available versus Power Required is a fundamental tool for assessing an aircraft's performance capabilities and overall dominance in flight. One significant aspect of this plot is the extent of excess power, which serves as a measure of the power available beyond what is required to maintain level flight. Excess power is a critical indicator of an aircraft's performance potential, as it represents the surplus power that can be utilized for various purposes such as acceleration, climbing, maneuvering, or overcoming adverse conditions.

A higher level of excess power indicates that the aircraft has a greater margin of performance superiority over other aircraft, allowing it to outperform competitors in terms of speed, agility, or maneuverability. Aircraft with significant excess power can execute dynamic maneuvers, achieve faster acceleration, and maintain higher speeds, giving them a strategic advantage in combat situations, air races, or other competitive scenarios.

Conversely, a lower level of excess power may limit an aircraft's performance capabilities, resulting in reduced maneuverability, slower acceleration, and inferior overall performance compared to competitors. Pilots and operators must carefully consider the amount of excess power available when assessing an aircraft's suitability for specific missions or operational requirements.

Understanding the extent of excess power depicted on the Power Available versus Power Required plot is crucial for pilots, operators, and mission planners as it informs strategic decisions regarding aircraft selection, mission planning, and tactical execution. By leveraging

excess power effectively, pilots can optimize aircraft performance, enhance operational capabilities, and gain a competitive edge in various flight scenarios.

Moreover, for aircraft designers and engineers, analyzing the relationship between power available and power required provides valuable insights into optimizing aircraft designs, propulsion systems, and performance characteristics to maximize excess power and overall performance capabilities. By designing aircraft with ample excess power, designers can ensure that aircraft possess the agility, speed, and maneuverability required to excel in diverse mission environments and operational scenarios.

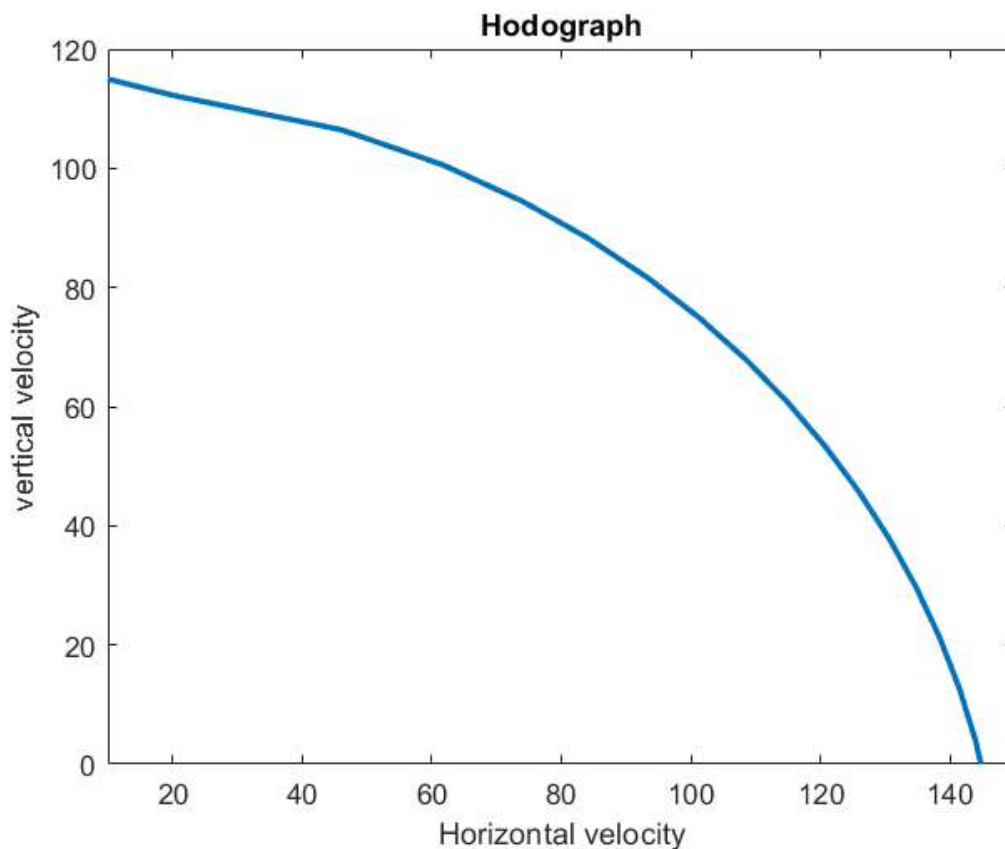


Figure 43 Hodograph for Gliding Flight

The Hodograph plot is indeed a significant tool in aircraft performance analysis, providing valuable insights into various parameters crucial for understanding and optimizing aircraft performance. This vertical versus horizontal velocity curve enables the calculation of several key parameters, including the maximum rate of climb, the rate of climb at the maximum climb angle (θ_{max}), the climb angle at the maximum rate of climb, and the maximum climb angle itself.

By examining the Hodograph plot, engineers and pilots can extract essential performance data necessary for flight planning, mission optimization, and aircraft design refinement. The maximum rate of climb represents the highest achievable climb rate for the aircraft under given conditions, indicating its ability to ascend rapidly. The rate of climb at θ_{max} provides insight into the aircraft's climb performance when flying at its optimal climb angle, which maximizes the altitude gain per unit of horizontal distance traveled.

Additionally, the Hodograph plot allows for the determination of the climb angle corresponding to the maximum rate of climb, providing critical information on the aircraft's climb efficiency and performance envelope. Furthermore, the plot facilitates the calculation of the maximum climb angle, representing the steepest angle at which the aircraft can ascend, which is essential for assessing its ability to clear obstacles or navigate challenging terrain during ascent.

Folding Mechanism

The UAV folding mechanism for a daughter plane, designed to be released from a parent cargo plane, requires careful engineering to ensure compactness, reliability, and ease of deployment. The mechanism should facilitate efficient folding and unfolding of the daughter plane's wings and other components, allowing it to transition seamlessly from a compact stowed configuration to a fully functional flight configuration.

One common approach is to incorporate hinge mechanisms at key joints of the daughter plane's structure, enabling the wings and other components to fold inward or outward as needed. These hinges should be robust and lightweight, constructed from durable materials such as high-strength aluminum or composite materials to withstand the forces and stresses encountered during flight and deployment.

Additionally, the folding mechanism may include locking mechanisms or latches to secure the wings and other components in both the folded and unfolded positions, preventing unintended movement during transport or flight. These locking mechanisms should be reliable and easy to engage and disengage, allowing for quick and efficient deployment of the daughter plane when required.

Furthermore, considerations should be given to the aerodynamic profile and structural integrity of the daughter plane in both folded and unfolded configurations. The folding mechanism should minimize drag and maintain the desired flight characteristics of the aircraft, while also ensuring that the structural integrity of the plane is not compromised during deployment or flight.

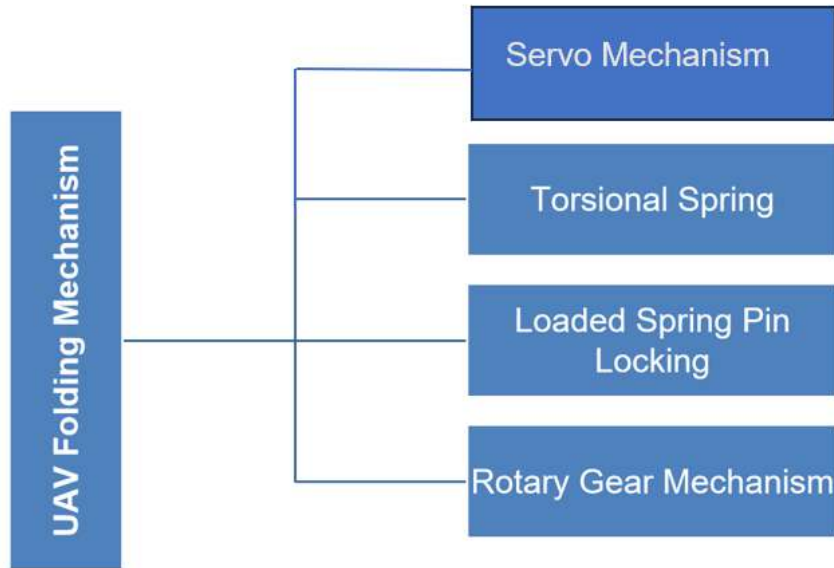


Figure 44 Wing Folding Mechanisms

Torsional Spring

Reason Of Failure:

- No Proper Locking of Wings
- Stiffness of Spring
- UAV Structure Limitation
- Rotation of Wings Along Lateral Axis
- Lack of Resources Locally Available

Loaded Spring

Reason of Failure

- Complex method to Install Springs
- Improper Locking of Parts
- Spring Stiffness and manufacturing constraints
- Big Assembly Size
- No locking Mechanism after Operated Once.

Spur Gear

Reason of Success

- Locking mechanism

- Manual / Autonomous control
- Electrically Actuated through Servo (PWM)
- Time to Open Mechanism (1.23 s)

Servo Operated Mechanism

Reason of Success

- Design Optimization for fuselage assembly.
- Locking mechanism
- Manual / Autonomous control
- Electrically Actuated through Servo (PWM)
- Adaptability
- Accuracy
- Accommodation of a range of payloads

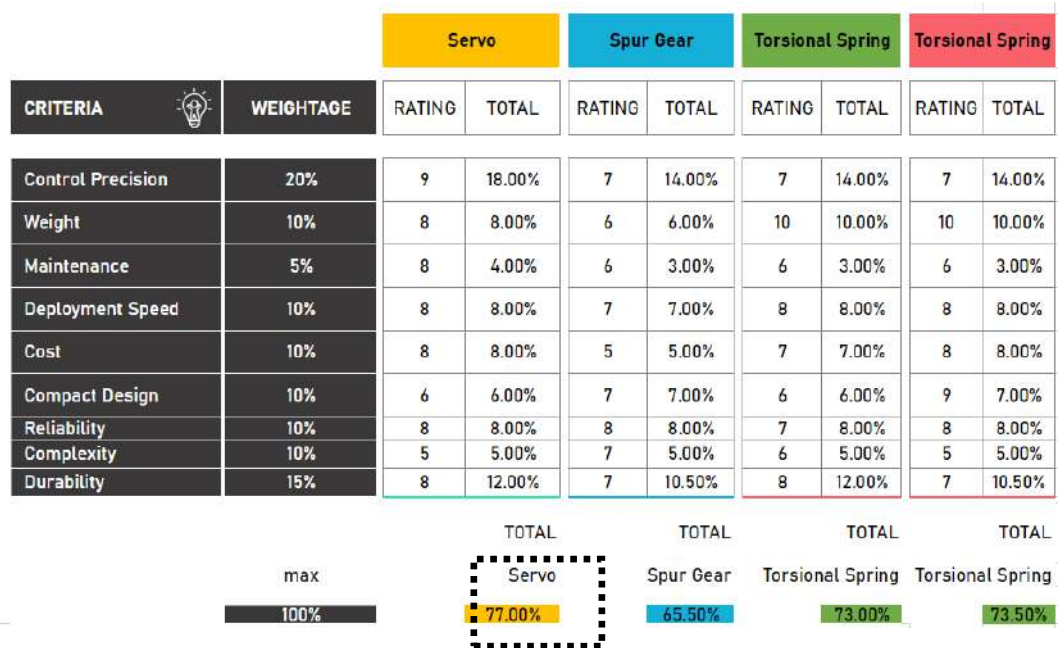


Figure 45: Weighted Matrix for Release Mechanism

Final CAD

Introduction to CAD Modelling using SolidWorks:

CAD (Computer-Aided Design) modelling is the process of creating digital representations of physical objects or systems. SolidWorks is powerful CAD software known for its parametric and feature-based modelling capabilities. CAD modeling using Solidworks is a versatile and powerful tool for creating detailed 3D models of mechanical and structural components, assemblies, and systems. The software offers a user-friendly interface and a wide range of features to facilitate the design and visualization process.

To begin CAD modeling in Solidworks, users typically start by creating a new part file or assembly file. Within the part file, various sketching tools are available to create 2D profiles that can be extruded, revolved, or lofted to generate 3D features. Solidworks provides a variety of sketch entities such as lines, arcs, circles, rectangles, and splines, allowing users to create complex geometries with ease.

Once the basic geometry is created, users can apply features such as extrusions, cuts, fillets, chamfers, holes, and patterns to modify and refine the part's shape and functionality. Solidworks also offers advanced modeling tools such as sweeps, lofts, ribs, shells, and surfaces for creating more complex and organic shapes.

For assemblies, users can create multiple parts and bring them together within an assembly file. Solidworks provides tools for mating components together using constraints such as coincident, concentric, parallel, and tangent, ensuring proper alignment and interaction between parts.

Solidworks also offers simulation capabilities for analyzing the performance of designs under various loading conditions, as well as tools for creating technical drawings, animations, and renderings to communicate design intent effectively.

Understanding SolidWorks Interface:

User Interface Overview:

The SolidWorks interface includes a ribbon-style toolbar with various tabs (e.g., File, Edit, Sketch) containing commands and tools. The central workspace is where 3D modelling occurs, and the left pane provides a feature tree to manage the model's history.

Parametric Modelling in SolidWorks:

Parametric modelling means creating 3D models by defining parameters (e.g., dimensions) and relationships (e.g., constraints) that govern the model's shape and behavior. Changes to these parameters automatically propagate throughout the model, ensuring design consistency.

Sketching and Feature-Based Modelling:

SolidWorks begins with sketching on 2D planes. Users draw 2D shapes (lines, circles, rectangles) and apply constraints (e.g., dimensions, relations) to define their size and position. Features (e.g., extrusions, cuts) are then applied to these sketches to create 3D geometry.

Creating 3D Models in SolidWorks:

Sketching and Constraints:

Sketches serve as the building blocks for 3D models. They are created on 2D planes and can be constrained with dimensions (e.g., length, angle) and relations (e.g., coincident, parallel) to define their shape and size accurately.

Extrusions and Revolves:

Extrusions add depth to sketches by pushing or pulling them in a specified direction. Revolves create 3D shapes by rotating a sketch profile around an axis. These operations convert 2D sketches into 3D objects.

Fillets and Chamfers:

Fillets round off sharp edges, while chamfers create beveled edges. These features improve both the aesthetics and functionality of a model, reducing stress concentrations and improving manufacturability.

Assembly Modelling:

Creating Assemblies:

Assemblies involve combining multiple parts (components) into a single unit. SolidWorks provides tools to create, arrange, and manage these components within an assembly.

Mate Relationships:

Mate relationships define how components within an assembly relate spatially to each other. Common mates include coincident (parts touch at a point or line), parallel (parts align along a common axis), and concentric (parts share the same center point).

Motion Studies and Simulations:

SolidWorks allows for motion studies to simulate how components within an assembly move. This can be valuable for testing mechanisms, assessing clearances, and detecting interferences.

Surface Modelling and Complex Geometry:

Surface Modelling Techniques:

Surface modelling is used when dealing with complex, freeform shapes that cannot be created with simple extrusions and revolves. Techniques such as lofts (connecting profiles), sweeps (swept along a path), and boundary features are employed.

Importing and Editing Surface Geometry:

SolidWorks allows the import of surface models created in other software. These imported surfaces can be edited and integrated into the existing SolidWorks design, facilitating collaboration and leveraging specialized tools.

Detailing and Drawing Creation:

Creating 2D Drawings:

SolidWorks generates 2D drawings from 3D models. These drawings include orthographic views (front, top, side), dimensions, annotations, and other details necessary for manufacturing and documentation.

Bill of Materials (BOM) and Exploded Views:

BOMs list the components of an assembly, along with quantities and part numbers. Exploded views show how parts are assembled step by step, aiding in assembly and maintenance.

Rendering and Visualization:

Photorealistic Rendering:

SolidWorks Visualize is a tool for creating high-quality, photorealistic renderings of 3D models. These visualizations are often used for presentations, marketing materials, and design reviews.

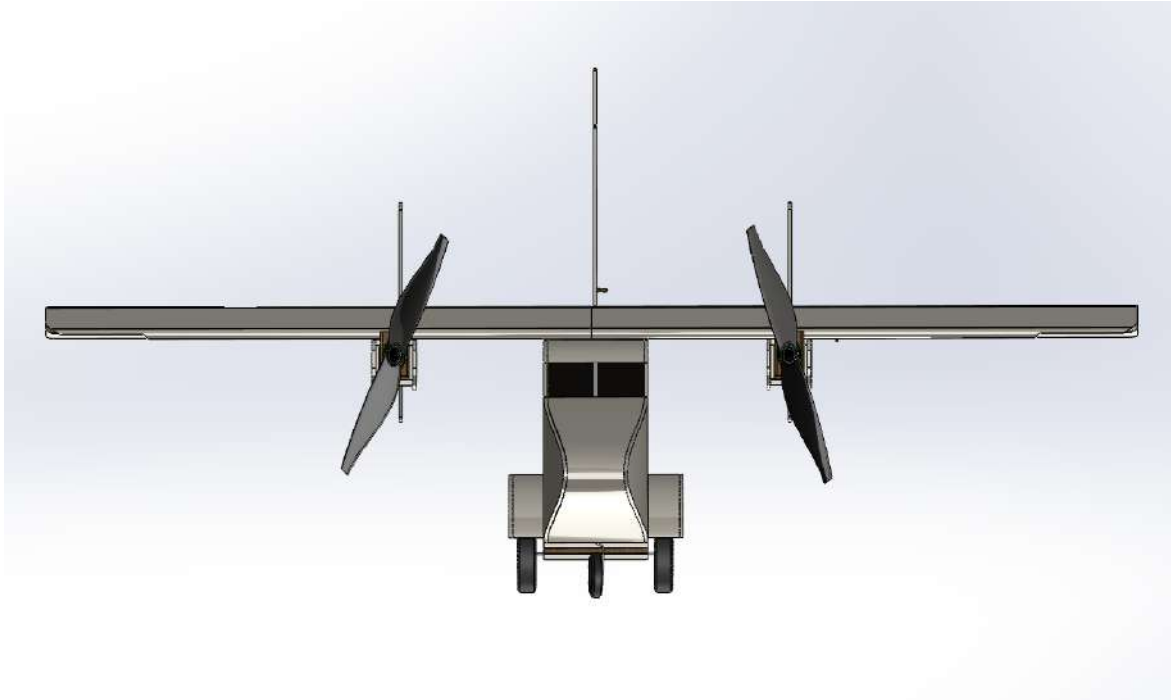


Figure 46 Front view of final CAD Model

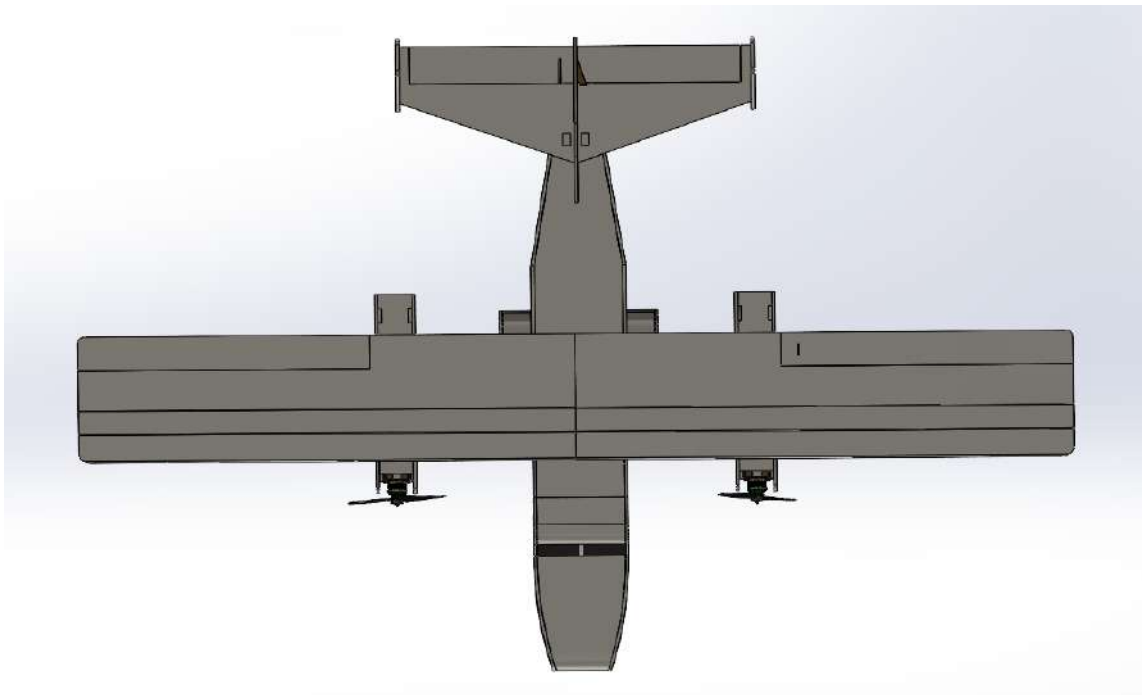


Figure 47: Top View of final CAD model.

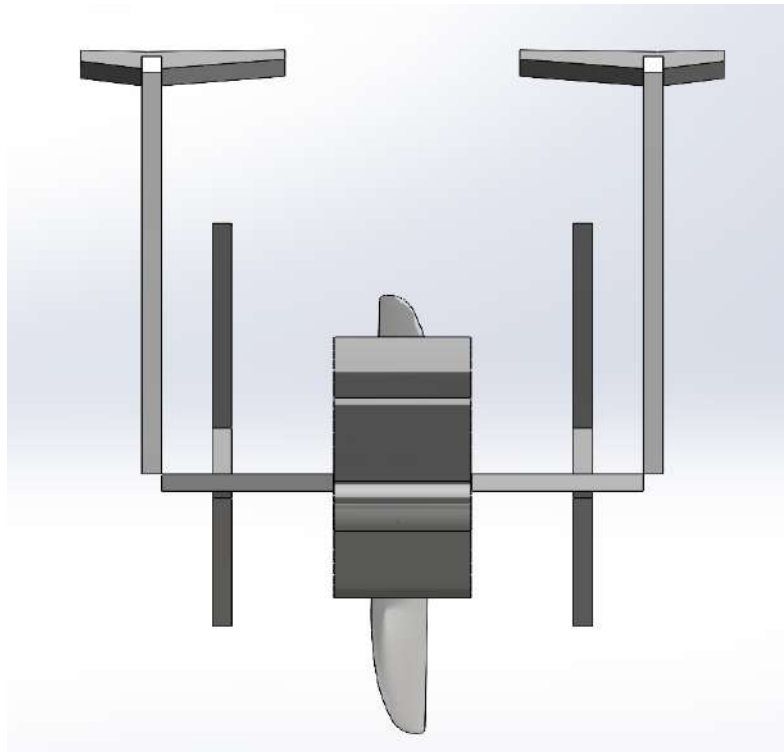


Figure 48: Completely Folded Wings of daughter UAV.

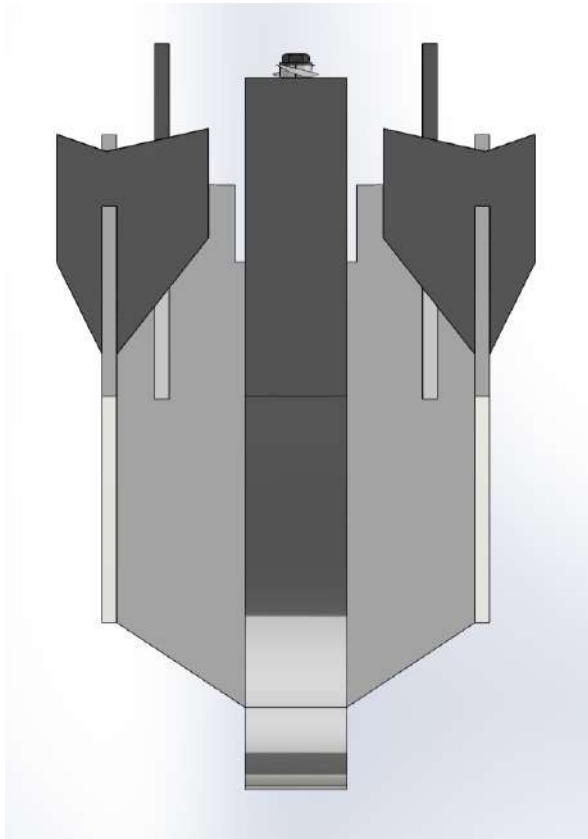


Figure 49: Top view of daughter UAV.

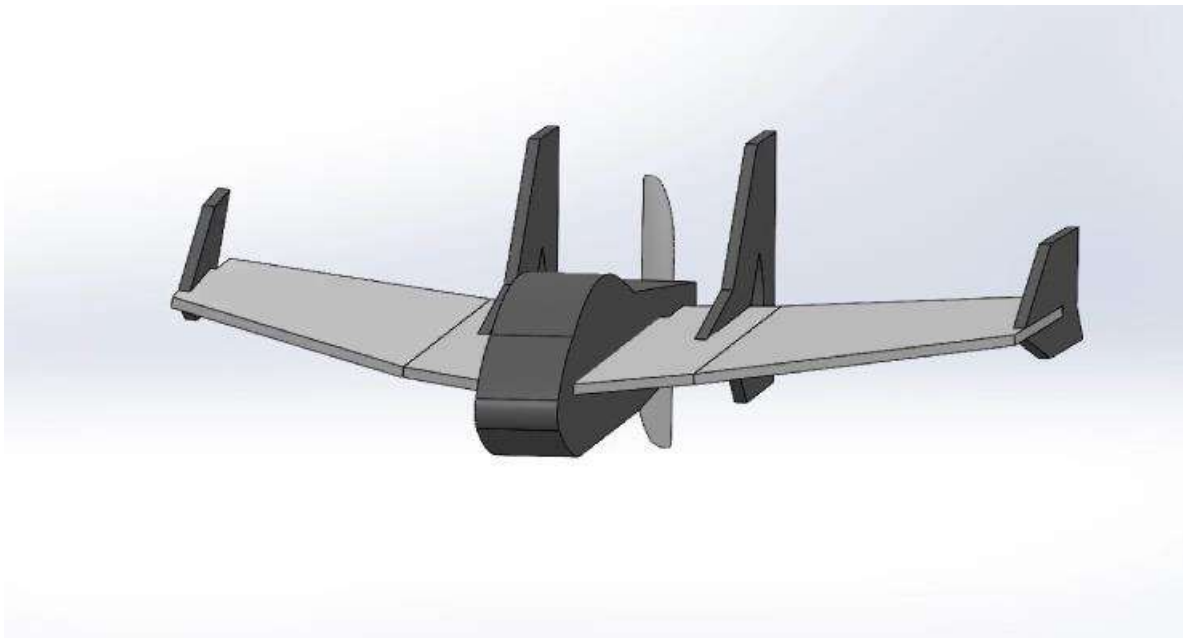


Figure 50: Unfolded daughter plane.

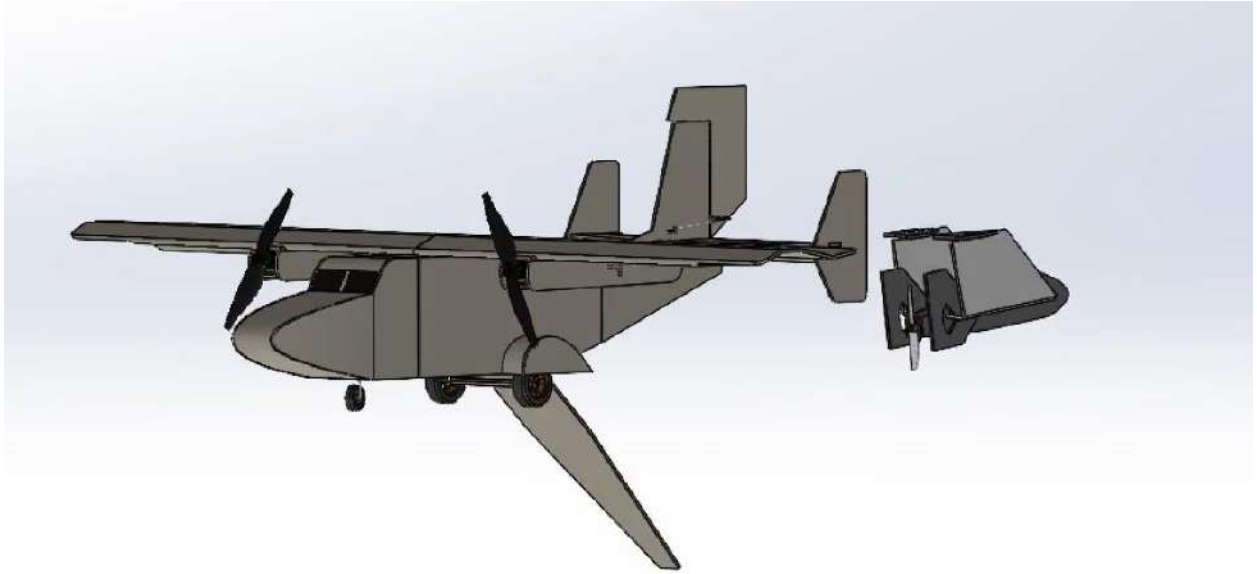


Figure 51: Inflight Separation Visualization

Prototype Development

Depron sheets, chosen as the material for manufacturing, offer a lightweight and versatile option ideal for a variety of applications in modeling and prototyping. Composed of expanded polystyrene foam, Depron sheets exhibit exceptional strength-to-weight ratio, making them suitable for crafting lightweight structures without compromising durability. The material's ease of cutting, shaping, and forming allows for intricate detailing and customization, facilitating the creation of complex designs and prototypes with precision. Additionally, Depron sheets boast excellent thermal and acoustic insulation properties, further enhancing their suitability for a range of applications. Whether used in the construction of model aircraft, architectural models, or hobby projects, Depron sheets provide a reliable and cost-effective solution for manufacturing lightweight structures with superior performance characteristics.

- Ease of manufacturing
- Complex Parts manufacturing
- Light weight
- Design Innovations
- Low-Cost Manufacturing

Fabricating both the parent and daughter planes involves a series of meticulous steps to ensure structural integrity, aerodynamic efficiency, and operational reliability. For the parent plane, the fabrication process typically begins with the construction of a lightweight yet sturdy airframe, often using materials like aluminum, carbon fiber, or composite materials. Precision machining techniques are employed to shape and assemble the fuselage, wings, empennage, and other structural components according to detailed engineering specifications. Advanced manufacturing methods such as CNC milling, 3D printing, and composite layup may be utilized to achieve the desired geometry and strength.



Figure 52: Fabricated Parts of Parent airplane.

Once the airframe is constructed, the parent plane undergoes rigorous testing and integration of avionics, propulsion systems, and payload accommodations. Avionics systems including flight control units, navigation systems, and communication equipment are carefully installed and calibrated to ensure seamless operation. Similarly, propulsion systems such as turbofan engines or turboprop engines are integrated, along with fuel systems and engine controls, to provide reliable thrust and power.



Figure 53: Control Surfaces positioning on fuselage.

For the daughter plane, the fabrication process is tailored to its unique requirements, particularly focusing on compactness, deployability, and aerodynamic

performance. Lightweight materials like carbon fiber, fiberglass, or Depron sheets may be used to construct the airframe, with emphasis on folding mechanisms and compact design to facilitate deployment from the parent plane. Detailed CAD modeling and simulation are employed to optimize the daughter plane's aerodynamic profile, folding mechanisms, and structural integrity.

Once both the parent and daughter planes are fabricated, extensive testing and validation procedures are conducted to ensure compliance with safety standards, performance requirements, and mission objectives. This includes ground testing, flight testing, and system integration tests to verify functionality, stability, and reliability under various operating conditions. Through a collaborative effort between engineers, technicians, and test pilots, the fabrication of the parent and daughter planes culminates in the production of sophisticated aerial platforms capable of fulfilling a wide range of missions with precision and efficiency.



Figure 54: Parents wing.



Figure 55:Fuselage for cargo parent airplane.



Figure 56:Fabricated parts for daughter plane

Flight Testing



Figure 57: Parent plane in spin.

During the inaugural flight of the parent plane, an unexpected tendency emerged wherein the aircraft exhibited a propensity to enter a spiral drop, a potentially hazardous situation that demanded immediate diagnosis and remediation. After thorough examination, the root cause of this phenomenon was determined to be asymmetric thrust, whereby one engine or propeller was generating more thrust than its counterpart. This imbalance in thrust distribution induced a yawing moment, resulting in the aircraft veering off its intended flight path and entering a spiral descent. To address this issue effectively, a comprehensive inspection of the aircraft was conducted, with particular attention focused on the propulsion system and wing configuration. Upon closer examination, it was discovered that the wings were not perfectly aligned with the direction of propeller rotation, contributing to the uneven distribution of thrust. As a corrective measure, adjustments were made to realign the wings to ensure they were parallel to the direction of propeller rotation, thereby mitigating the effects of asymmetric thrust. Furthermore, additional measures were implemented to balance the thrust output of the propulsion system, such as fine-tuning engine settings, adjusting propeller pitch, or recalibrating engine controls. These adjustments aimed to achieve uniform thrust distribution across all engines or propellers, minimizing the yawing moment and restoring stability to the aircraft during flight.

Following these modifications, the parent plane underwent rigorous ground testing and flight testing procedures to validate the effectiveness of the corrective measures. Through meticulous

testing and validation, the aircraft's performance was closely monitored, and adjustments were made as necessary to ensure optimal stability and control.

Ultimately, by diagnosing the issue of asymmetric thrust and implementing appropriate adjustments to the wing configuration and propulsion system, the parent plane was able to overcome its tendency to enter a spiral drop, ensuring safe and stable flight operations for future missions. This experience underscored the importance of thorough inspection, diagnosis, and proactive measures in addressing unexpected challenges encountered during flight testing and aircraft development processes.



Figure 58: Daughter plane in Roll.

During the maiden flight of the daughter plane, an unexpected tendency of roll was observed, attributed to the overwhelming torque generated by the motor. This phenomenon posed a significant challenge to the aircraft's stability and control, necessitating prompt diagnosis and intervention to ensure safe and effective flight operations. Upon thorough examination and analysis, it was determined that the excessive motor torque was inducing an uncommanded rolling motion, adversely affecting the aircraft's flight path and maneuverability.

To address this issue effectively, a comprehensive solution was devised, focusing primarily on modifying the propulsion system to produce the required thrust while mitigating excessive torque. As a first step, the existing motor and propeller combination were evaluated to identify alternatives that could deliver the necessary thrust without overwhelming torque effects. Subsequently, a suitable replacement motor and propeller combination were selected based on their ability to provide adequate thrust while maintaining manageable torque levels.

Once the new motor and propeller were procured, they were carefully installed and integrated into the daughter plane's propulsion system, ensuring proper alignment and configuration to

optimize performance and minimize adverse effects on aircraft stability. Additionally, adjustments to motor settings, such as throttle response and power output, were made to fine-tune the system and achieve the desired balance between thrust and torque.

Following the implementation of these modifications, the daughter plane underwent comprehensive ground testing and flight testing procedures to validate the effectiveness of the solution and ensure the aircraft's stability and control under various operating conditions. Through meticulous testing and validation, any remaining issues or concerns were addressed, and adjustments were made as necessary to optimize performance and ensure safe and reliable flight operations.

Ultimately, by diagnosing the issue of overwhelming motor torque and implementing appropriate modifications to the propulsion system, the daughter plane was able to overcome its tendency of uncommanded rolling motion, ensuring stable and controlled flight operations for future missions. This experience underscored the importance of proactive problem-solving and thorough testing in addressing unexpected challenges encountered during the development and testing of aircraft systems.

Challenges and Possible reasons

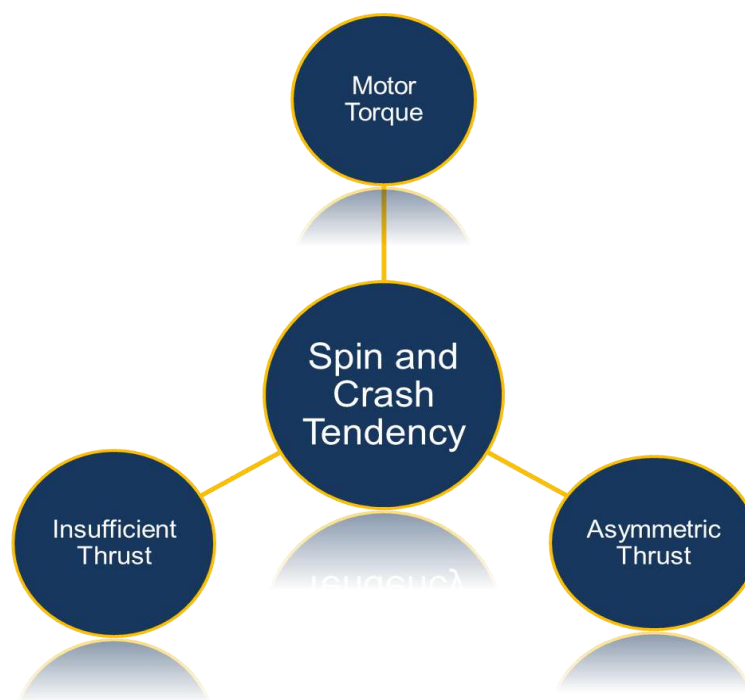


Figure 59 Challenges faced during development.

Indeed, the successful operation of any aircraft, whether it be a parent plane or a daughter plane, relies heavily on identifying and addressing any issues that arise during flight testing. Each problem encountered during flight testing presents a unique set of challenges that must be diagnosed accurately and catered to effectively to ensure safe and successful flights in the future.

For instance, in the case of the parent plane experiencing a tendency to enter a spiral drop due to asymmetric thrust, a thorough inspection of the aircraft's propulsion system and wing

configuration was conducted. The root cause of the issue was identified, and corrective measures such as realigning the wings and balancing the thrust output were implemented. This allowed the parent plane to regain stability and control during flight, paving the way for successful missions.

Similarly, when the daughter plane exhibited a tendency to roll due to overwhelming motor torque during its first flight, a comprehensive solution was devised to address the issue. By selecting a suitable replacement motor and propeller combination and making adjustments to the propulsion system settings, the excessive torque effects were mitigated, restoring stability and control to the aircraft.

In both cases, the diagnostic process involved a systematic approach that included careful analysis of flight data, thorough inspections of aircraft components, and collaboration among engineers, technicians, and test pilots. Once the root causes of the problems were identified, appropriate corrective actions were taken, followed by extensive ground testing and flight testing to validate the effectiveness of the solutions.

Through this iterative process of diagnosis and problem-solving, the parent and daughter planes were able to overcome their respective challenges and move towards successful flights. These experiences underscore the importance of proactive problem identification and resolution in ensuring the safety, reliability, and performance of aircraft systems, ultimately contributing to the success of missions and operations.

Flights after applying correction.



Figure 60: Successful flight of Parent plane.



Figure 61: Successful flight of daughter plane.

Multitasking Operations

After successful flights exhibition, the project proceeded towards the multitasking part. Following is the list of multitasking operation that can be done with the CC-UAV:-

Deception

In a scenario where the CC-UAV is deployed into a potentially hostile territory, the threat of detection, both visually and acoustically, poses a significant challenge to the success of the mission. However, with careful planning and strategic deployment tactics, the CC-UAV can leverage the element of surprise and its multitasking capabilities to maintain operational effectiveness in the face of adversarial threats.

As the CC-UAV is transported within the belly of the parent plane, it remains concealed from visual and acoustic detection, providing a stealthy approach to the mission area. This covert deployment strategy allows the CC-UAV to evade enemy surveillance and reconnaissance efforts, minimizing the risk of detection and interception before reaching the target area.

Within the parent plane's cargo hold, the daughter drone remains on standby, ready to be deployed at a moment's notice in response to any detected threats or emerging opportunities. Equipped with its own suite of sensors, communication systems, and payload capabilities, the daughter drone serves as a versatile asset capable of performing a wide range of tasks independently or in coordination with the parent plane.

Upon detecting visual or acoustic signals indicative of hostile presence, such as enemy patrols, surveillance equipment, or anti-aircraft defenses, the CC-UAV's onboard sensors and intelligence-gathering capabilities come into play. Real-time data analysis and threat

assessment algorithms enable the CC-UAV to identify potential threats and determine the appropriate course of action.

In response to detected threats, the CC-UAV has the option to deploy the daughter drone as a diversionary tactic or to continue the mission autonomously while the parent plane maintains a safe distance or retreats to avoid confrontation. The daughter drone's smaller size and agility make it well-suited for evasive maneuvers and reconnaissance missions in contested airspace, allowing it to gather critical intelligence or engage enemy targets as necessary.

Alternatively, if the threat level is deemed manageable, the parent plane and daughter drone may opt to coordinate their efforts, with the parent plane providing support and cover for the daughter drone's mission objectives. This collaborative approach enables the CC-UAV to maximize its operational effectiveness and achieve mission success while mitigating risks and preserving resources.



Figure 62: Internal view during drop.

Reconnaissance

The CC-UAV represents a cutting-edge solution for reconnaissance operations, characterized by its swift deployment, foldable design, and advanced sensor capabilities. Designed to excel in navigating diverse terrains and operating independently, the mini plane is equipped to provide crucial situational awareness and real-time data acquisition for both tactical and strategic reconnaissance missions in dynamic operational scenarios.

One of the key strengths of the CC-UAV lies in its swift deployment capability, facilitated by its foldable design. This feature enables the UAV to be easily transported and rapidly deployed into the field, allowing for quick response to emerging threats or intelligence requirements. Whether deployed from a parent aircraft or launched from a ground-based platform, the CC-

UAV can be ready for action within minutes, providing operators with immediate access to critical intelligence and surveillance capabilities.

Once deployed, the CC-UAV leverages its advanced sensor suite and camera systems to enhance situational awareness and gather real-time data from the operational environment. Equipped with high-resolution cameras, infrared sensors, and other specialized sensors, the UAV is capable of capturing detailed imagery and detecting key indicators such as enemy movements, infrastructure changes, or environmental conditions.

The versatility of the CC-UAV's sensor capabilities allows it to adapt to a wide range of reconnaissance tasks, from tactical surveillance of enemy positions to strategic mapping of terrain features or infrastructure assets. Whether conducting low-altitude patrols or high-altitude aerial surveys, the UAV provides operators with valuable insights into the operational environment, enabling informed decision-making and mission planning.

In addition to its reconnaissance capabilities, the CC-UAV's autonomous navigation features further enhance its operational effectiveness. With the ability to navigate autonomously using GPS waypoints or follow pre-programmed flight paths, the UAV can cover large areas efficiently and effectively, reducing the workload on operators and maximizing mission coverage.



Figure 63: Surveilling View.

Suicide drone.

The concept of utilizing the daughter drone as a suicidal drone, akin to the kamikaze tactic, involves equipping the UAV with a payload intended to neutralize a target by colliding with it. While such a tactic is inherently high-risk and carries ethical considerations, it may be deemed necessary in certain scenarios where traditional means of neutralizing a target are not feasible or pose unacceptable risks to personnel or assets.

In this context, the daughter drone is outfitted with a specialized payload designed to maximize the impact upon collision with the target. This payload could vary depending on the nature of the mission and the target being engaged. Examples of payloads may include explosives, high-

speed projectiles, or other kinetic energy-based weapons designed to inflict maximum damage upon impact.

The decision to employ the daughter drone as a suicidal drone must be made judiciously, weighing the potential benefits against the inherent risks and ethical considerations. Factors such as the nature of the target, the level of threat posed, and the availability of alternative means of neutralization should all be carefully considered before implementing such a tactic.

From a tactical standpoint, the suicidal drone tactic offers several potential advantages. It allows for precision targeting and engagement of high-value or heavily defended targets, bypassing traditional defenses and potentially catching adversaries off guard. Additionally, the speed and agility of the daughter drone enhance its ability to penetrate enemy defenses and deliver its payload with accuracy and effectiveness.

However, there are also significant risks and ethical concerns associated with employing suicidal drones. The loss of the UAV as a result of the collision may represent a substantial financial investment, and there is also the risk of collateral damage or unintended consequences resulting from the attack. Furthermore, the use of suicidal drones raises ethical questions regarding the principles of proportionality, necessity, and the protection of non-combatants.

In conclusion, while the concept of utilizing the daughter drone as a suicidal drone offers potential tactical advantages in certain scenarios, it must be approached with caution and careful consideration of the associated risks and ethical implications. Ultimately, decisions regarding the use of such tactics should be guided by a thorough assessment of the operational context and adherence to principles of international law and ethical conduct.

Cargo drone

Parent plane can also be utilized for a suicidal daughter drone drop or fitted with payload that can be dropped where the explosion is needed. Parent plane can be incorporated with 300g payload for explosion or supply drop.



Figure 64: Austria HG 86 Mini

Payload	Daughter plane	Austria HG 86 Mini
Weight	240g	180g
Purpose	Reconnaissance, suicidal drone	Explosive grenade
Size	Length: 355.6 mm Width: 127 mm	Length 76 mm Diameter 43 mm

CONCLUSIONS AND FUTURE WORK

Conclusion

The tandem wing design, coupled with low-cost Fused Deposition Modeling (FDM) manufacturing techniques, offers a promising combination for the development of versatile unmanned aerial vehicles (UAVs) capable of both autonomous and manual flight operations.

The tandem wing configuration, characterized by two wings positioned one behind the other along the longitudinal axis of the aircraft, offers several advantages over traditional monoplane designs. One key benefit is enhanced stability and control, achieved through the distribution of lift across multiple wing surfaces. This configuration also allows for efficient aerodynamic performance, reducing drag and increasing overall efficiency, particularly at high angles of attack. Additionally, the tandem wing layout offers flexibility in payload placement and integration, accommodating various mission-specific equipment and sensors while maintaining optimal aerodynamic performance.

Complementing the tandem wing design is the utilization of low-cost FDM manufacturing techniques, which enable the rapid prototyping and production of lightweight yet durable UAV components. FDM involves the layer-by-layer deposition of thermoplastic materials, such as ABS or PLA, to create complex geometries with high precision and accuracy. This manufacturing method offers significant cost savings compared to traditional manufacturing processes, making it ideal for the production of UAVs for commercial, research, and educational purposes. Additionally, the availability of desktop FDM printers further enhances accessibility and scalability, allowing for decentralized manufacturing and customization of UAV components to meet specific mission requirements.

The incorporation of both autonomous and manual flight capabilities further enhances the versatility and utility of UAVs utilizing tandem wing design and low-cost FDM manufacturing. Autonomous flight features, enabled by onboard sensors, GPS, and advanced flight control systems, allow for precise navigation, waypoint following, and mission planning without direct human intervention. This capability is particularly valuable for tasks such as aerial mapping,

surveillance, and environmental monitoring, where long-duration, repeatable missions are required.

Conversely, manual flight capabilities provide operators with real-time control and situational awareness, enabling dynamic mission adjustments, obstacle avoidance, and emergency response. Manual control modes allow operators to take direct control of the UAV's flight path and maneuverability, providing flexibility in response to changing mission requirements or unexpected events. This dual-mode capability ensures adaptability and resilience in the face of diverse operational challenges and environments.

Future Work

The integration of autonomous flight capabilities using a flight controller, coupled with the implementation of a target detection system for counter-counter UAV operations, computational fluid analysis (CFA) for improved drone drop and design, and analysis using toroidal propellers, represents a comprehensive approach to enhancing the functionality, efficiency, and performance of unmanned aerial vehicles (UAVs) across a variety of applications.

Autonomous flight using a flight controller is a fundamental component of modern UAV technology, enabling precise navigation, waypoint following, and mission execution without direct human intervention. A flight controller is a small electronic device that integrates sensors, processors, and algorithms to stabilize and control the UAV's flight, adjusting motor speeds, control surfaces, and other parameters to maintain stability and achieve desired flight paths. By leveraging advanced sensors such as GPS, accelerometers, gyroscopes, and magnetometers, along with sophisticated control algorithms, autonomous flight capabilities enable UAVs to perform complex tasks with accuracy and reliability, including aerial mapping, surveillance, and delivery operations.

In addition to autonomous flight, the utilization of a target detection system enhances the UAV's capabilities for counter-counter UAV operations, allowing it to detect, track, and neutralize hostile UAV threats. Target detection systems typically integrate sensors such as cameras, radar, lidar, or radio frequency (RF) scanners to identify and classify potential threats in the airspace. Advanced image processing algorithms and machine learning techniques further enhance the system's ability to distinguish between friendly and hostile UAVs, enabling rapid response and engagement when necessary.

Computational fluid analysis (CFA) is a powerful tool for optimizing drone drop and design, allowing engineers to simulate and analyze the aerodynamic performance of UAVs in various operating conditions. By modeling airflow around the UAV's fuselage, wings, and other components, CFA enables engineers to identify areas of drag, turbulence, or inefficiency and iteratively refine the design to improve aerodynamic efficiency, stability, and performance. This iterative design process helps minimize energy consumption, extend flight endurance, and enhance overall flight characteristics, resulting in more agile, responsive, and efficient UAVs. Lastly, analysis using toroidal propellers introduces a novel approach to propulsion systems, leveraging the unique aerodynamic properties of toroidal (doughnut-shaped) propellers to improve efficiency, thrust, and maneuverability. Unlike traditional propeller designs, which generate thrust primarily through axial airflow, toroidal propellers create a vortex ring effect

that enhances lift generation and reduces drag, resulting in improved overall efficiency and performance. By optimizing the shape, size, and rotation speed of toroidal propellers through computational modeling and testing, engineers can develop UAV propulsion systems that offer superior performance, stability, and control across a wide range of operating conditions.

```
clc

close all

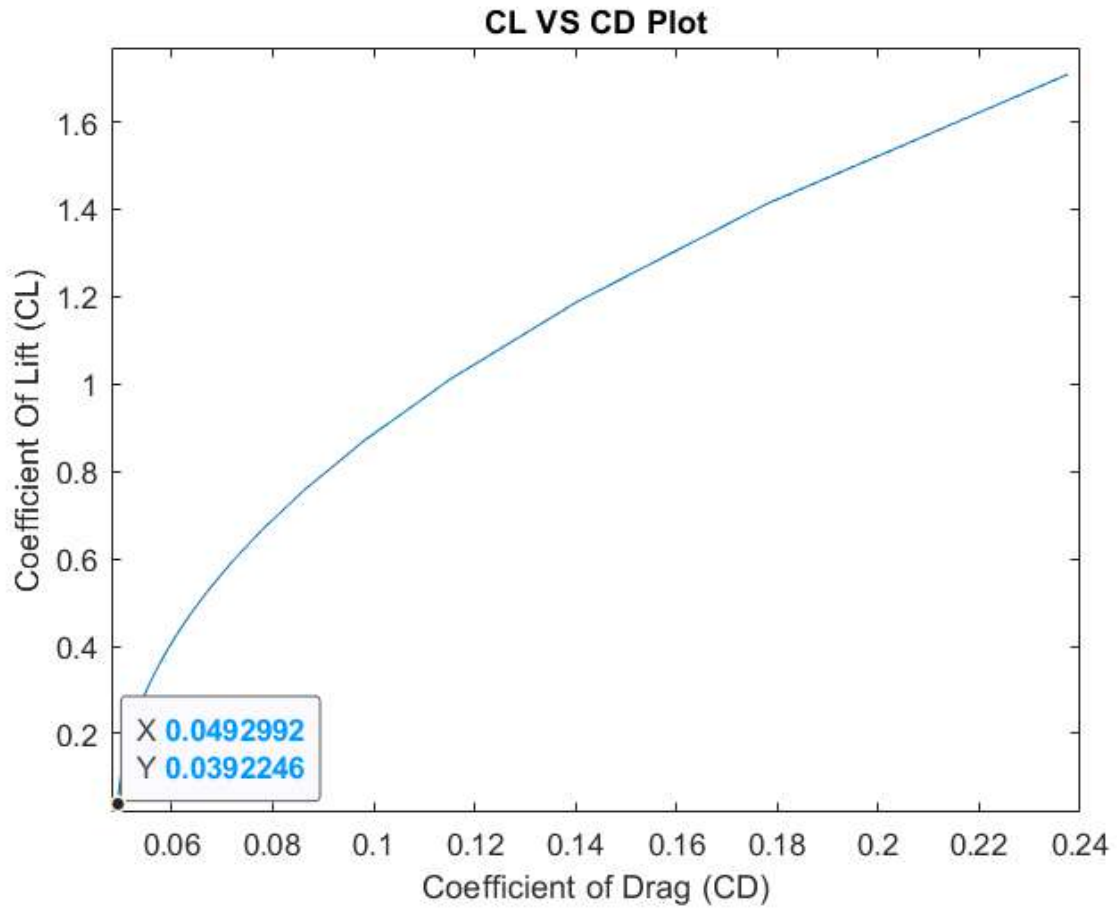
AR = 4.66.
%Assuming a span efficiency factor of (e=0.9)
e=0.94.
k3=1/((pi)*(e)*(AR)).
% Since k2 =0 no wave drags subsonic aircraft %
k1=k3/3.
K=k1+k3.
% Calculating Drag Polar
%Assuming a span efficiency factor of (e=0.9)
% From Given reference value of (Cd, o =0.011) %
% Equation of drag polar Cd=Cd, o + K(CL)^2 %

W= 5.29; %lbs
Rho=0.002377; %slugs/ft^3
Vel=45:2:183; %ft/s

%Calculating Lift coefficient
% Wingspan S=1.1302 sq. ft
S=1.1302; % Sq.ft
q = 0.5*Rho*Vel.^2.
% Calculating Drag Polar
% Coefficient of lift for steady level flight
Cl = (2*W). / (Rho*(Vel.^2) *S);

CD_Knot= 0.0492.
CD=CD_Knot+K.*(Cl). ^2.

plot (CD, Cl)
ylabel ('Coefficient of Lift')
xlabel ('Coefficient of Drag')
title ('CL VS CD Plot')
```



```

% Zero-Lift Thrust required
Zero_Lift_Drag = q*S*CD_Knot.

% Thrust required due to lift
Drag_Dueto_Lift = S*K.*q.*Cl.^2.

% Total Thrust Required
Thrust_Req = Zero_Lift_Drag + Drag_Dueto_Lift.

plot (Vel, Zero_Lift_Drag, 'g')

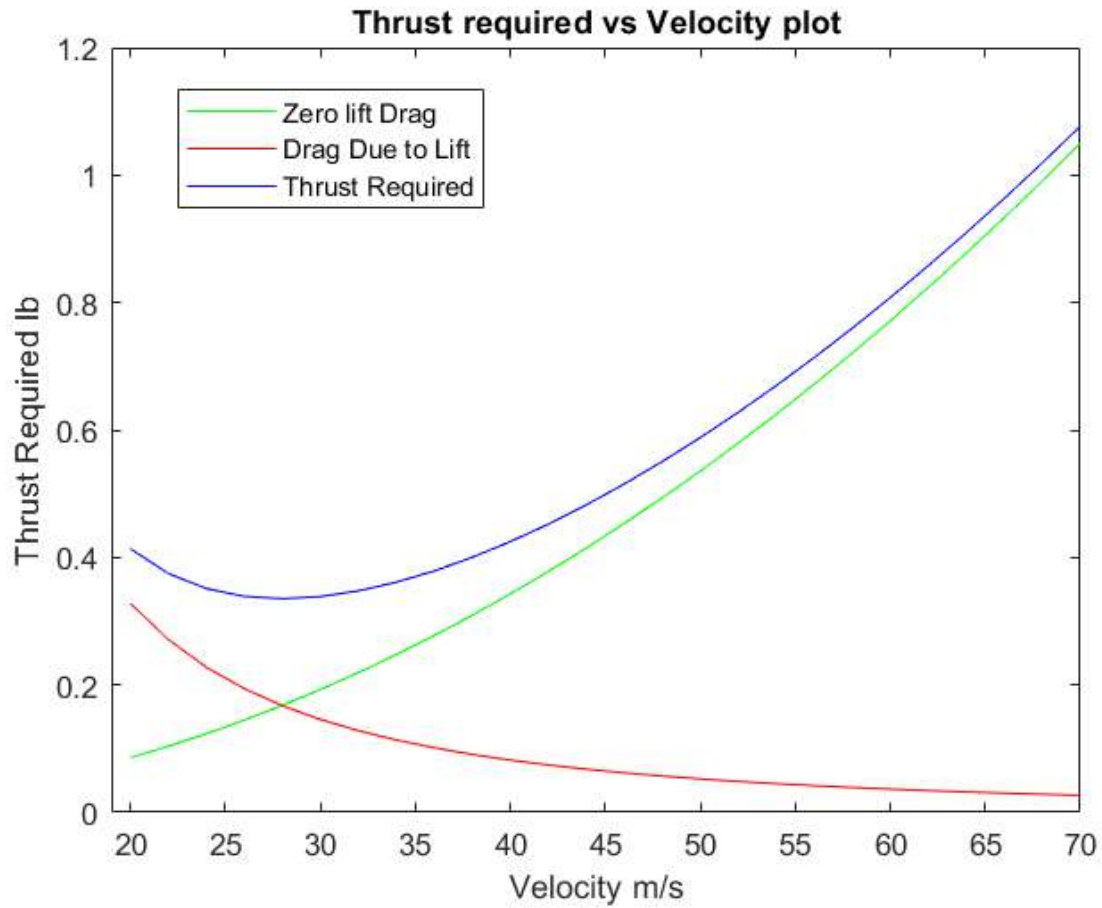
hold on.

plot (Vel, Drag_Dueto_Lift, 'r')
hold on.

plot (Vel, Thrust_Req, 'b')
hold off.
P_r=Thrust_Req.*Vel.
b = convvel (Vel, 'ft/min', 'm/s').

xlabel ('Velocity m/s')
ylabel ('Thrust Required lb')
title ('Thrust required vs Velocity plot')

```



```

%Minimum Thrust Required
% Following the data and Results in above section
%calculating Thrust Required
TR_min=(W) * (4*CD_Knot*K) ^0.5.

```

Wing Loading

```

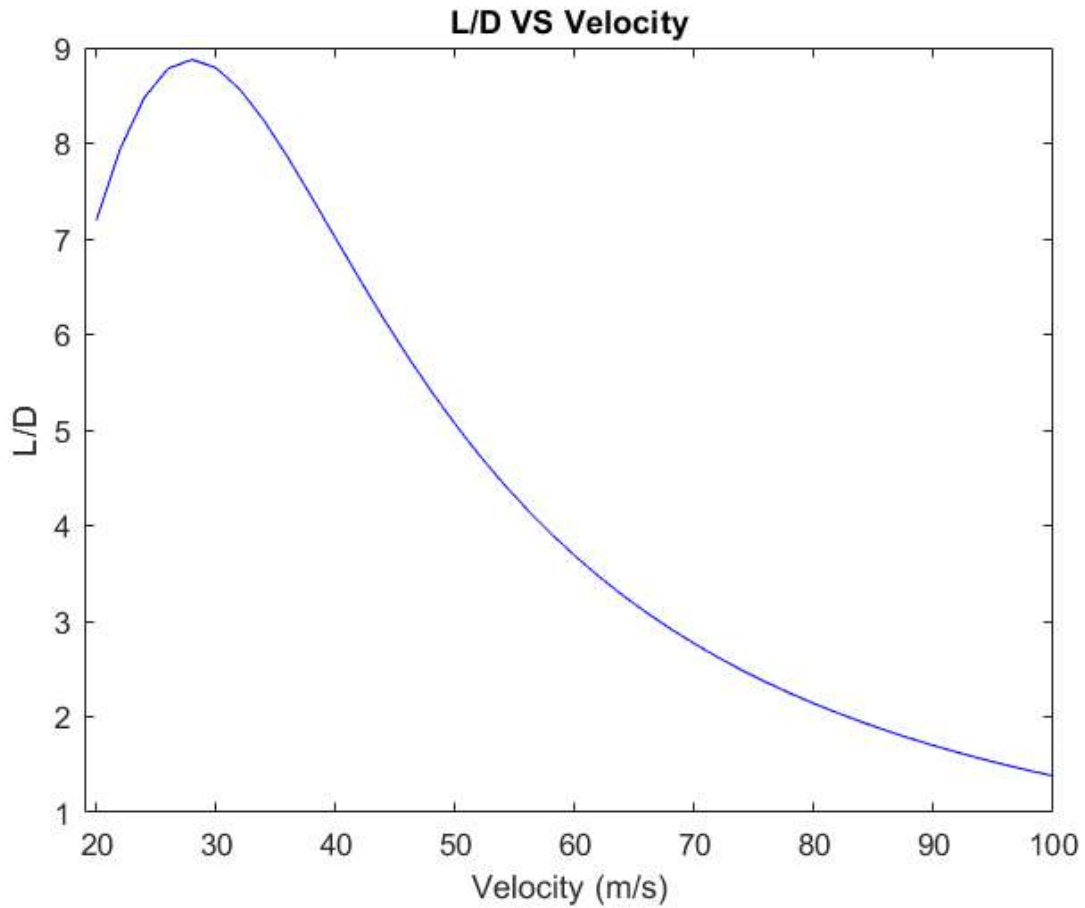
Wing_Loading=(W) / (S) .

% velocity at minimum Thrust
V_Tr_min=((2) / (Rho) * (sqrt(K/CD_Knot)) * (Wing_Loading)) ^0.5;
%L by D, L by D max
%Following the data and Results in above section
% for L/D
L_D= (((Rho. * (Vel.^2)
*CD_Knot) ./ (2*Wing_Loading)) + ((2*K*Wing_Loading) ./ (Rho.*Vel.^2))) .^-1;

plot (Vel, L_D, 'b')
xlabel ('Velocity')
ylabel ('L by D')
title ('L by D VS Velocity Plot ')

L_D_max=max(L_D) .

```



```

%Aerodynamic Relations
% Calculation Of CL/CD, (CL^3/2)/CD, (CL^1/2)/CD

        % CL/CD max    and Velocity at CL/CD max
CL_by_CD=Cl./CD.
CL_by_CD_max=7.2407.
V_CL_CD_max=((2/Rho) *(sqrt(K/CD_Knot) *(Wing_Loading)) ^0.5).
plot (Vel, CL_by_CD,'g')
hold on.

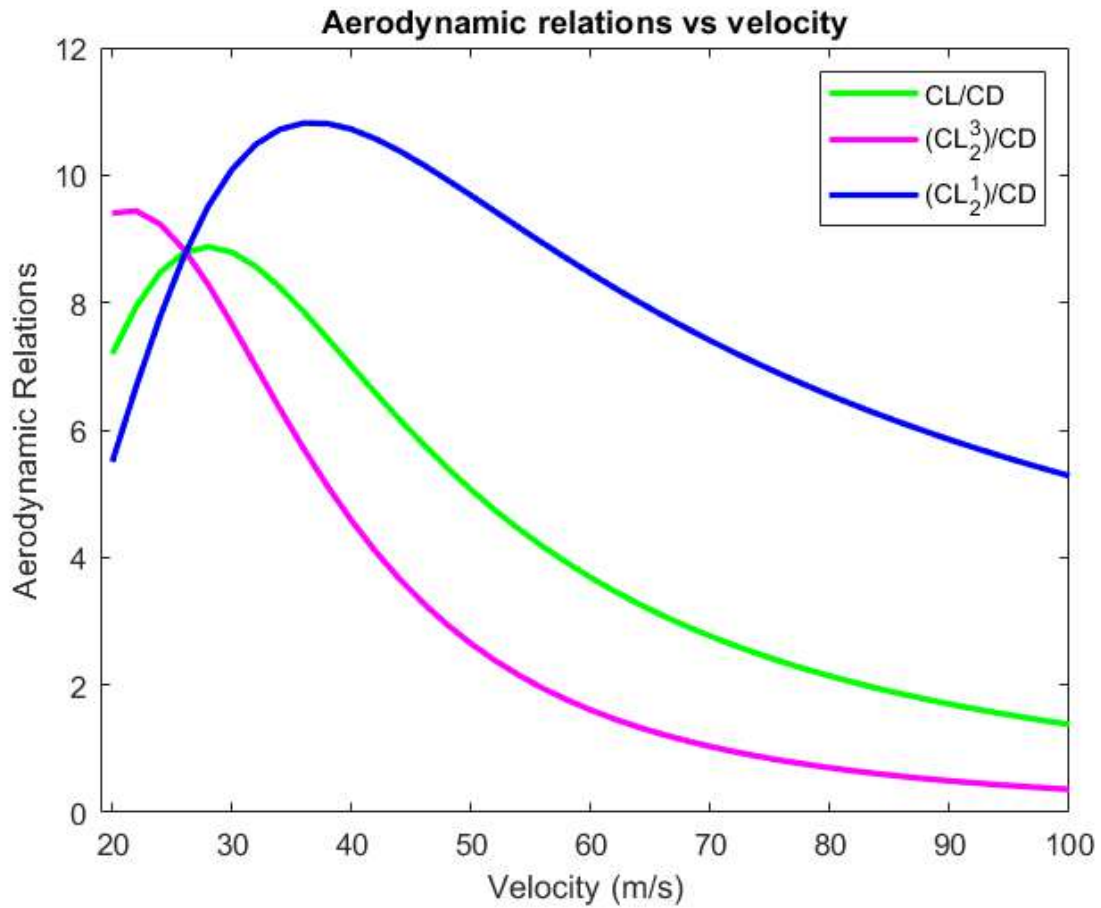
        % CL^3/2 /CD max    and Velocity at CL ^3/2 / CD max
CL_3_2_by_CD=(Cl) . ^1.5. /CD.
CL_3_2_CD_max = (1/4) *((3/ (K*(CD_Knot^ (1/3)))) ^ (3/4));
V_CL_3_2_CD_max = V_CL_CD_max/ (3^(1/4)).
plot (Vel, CL_3_2_by_CD,'m')
hold on.

        % CL^1/2 /CD max    and Velocity at CL ^1/2 / CD max
CL_1_2_by_CD=(Cl) . ^0.5./CD;

CL_1_2_CD_max = (3/4) *(1/(3*K*(CD_Knot^3)))^(1/4);
V_CL_1_2_CD_max = (3^(1/4))*V_CL_CD_max;
plot (Vel, CL_1_2_by_CD,'b')
hold off.

xlabel('Velocity')
ylabel ('Aerodynamic Relations')
title ('Aerodynamic relations vs velocity')

```

```
%Computing Drag due to lift and zero lift drag
```

```
    % At CL_3_2_CD_max
```

```
% Finding Dynamic pressure
```

```
q= ((0.5) *(Rho)*(V_CL_3_2_CD_max^(2)));
```

```
% Zero lift Drag
```

```
CL_new=((W)/(q*S)).
```

```
Zero_lift_drag=q*S*CD_Knot.
```

```
Drag_due_to_lift=q*S*K*(CL_new^2).
```

```
% comparing both lifts
```

```
R=(Zero_lift_drag)/(Drag_due_to_lift).
```

```
    % At CL_1_2/CD
```

```
q_1= ((0.5) *(Rho)*(V_CL_1_2_CD_max^(2)));
```

```
% Zero lift Drag
```

```
CL_new_1=((W)/(q_1*S)).
```

```
Zero_lift_drag=q_1*S*CD_Knot.
```

```
Drag_due_to_lift=q_1*S*K*(CL_new_1^2).
```

```
% comparing both lifts
```

```
R_1=(Zero_lift_drag)/(Drag_due_to_lift).
```

```
    % At CL/CD
```

```
q_2= ((0.5) *(Rho)*(V_CL_CD_max^(2)));
```

```

% Zero lift Drag
CL_new_1=((W)/(q_2*S)) ;

Zero_lift_drag=q_2*S*CD_Knot.
Drag_due_to_lift=q_2*S*K*(CL_new_1^2).

% comparing both lifts
R_2=(Zero_lift_drag)/(Drag_due_to_lift).

%Using Graphical approach to find V_max

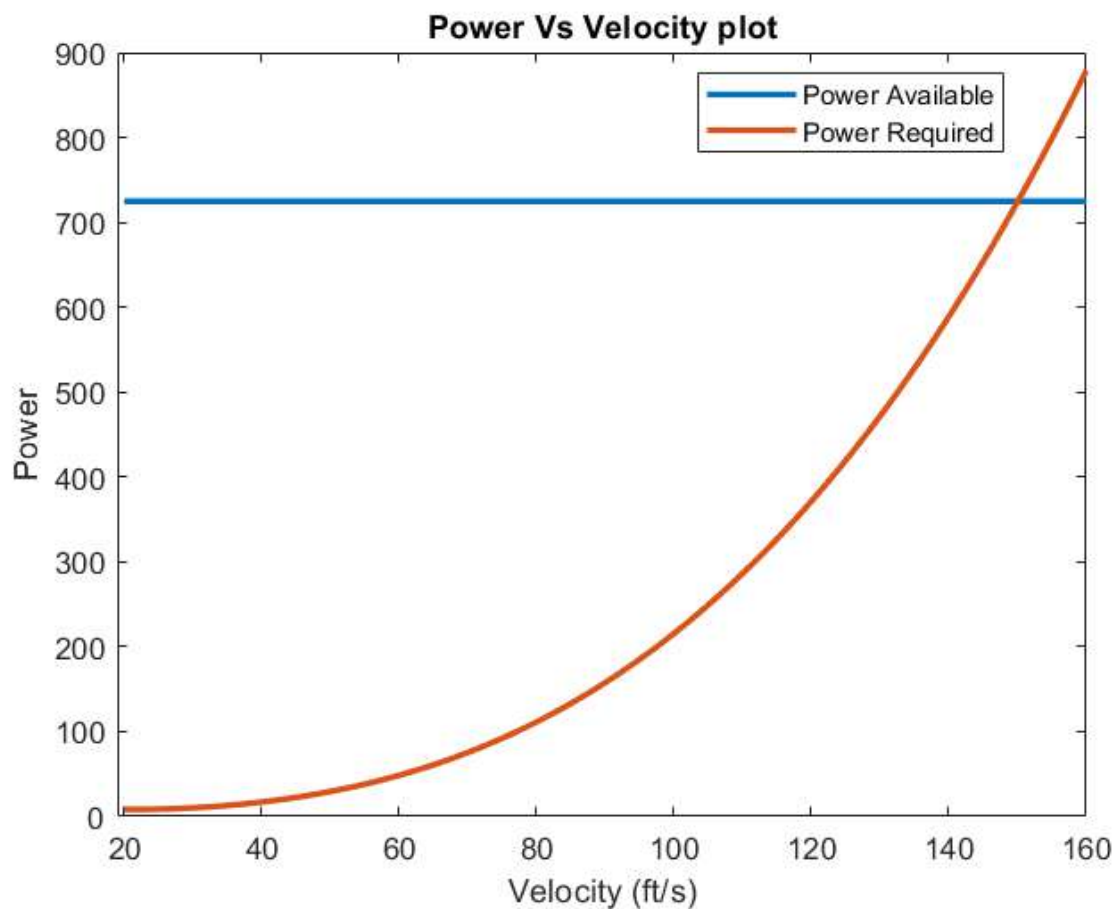
% Intersection of Power available and power required gives the V_max
%power available for propeller aircraft remains constant with altitude
% AS2820 1250kv long shaft
% Power 1092W
Shaft_power=805.41; %lb.ft/s

npr=0.9.
P_Available=(Shaft_power) *npr.

plot (Vel, Vel*0+P_Available,'g')
hold on.
P_Req=P_r.

plot (Vel,P_Req,'c')
hold off.
xlabel('Velocity')
ylabel('Power')
title ('Power Vs velocity plot for Vmax , L by D, Power Req min')

```



```

%Stall velocity
% For the calculation of V_Stall
% Using airfoiltools.com for airfoil is HQ-358
% Cl_max from graph is 1.22
CL_max=1.22.
V_stall = sqrt((2*W)/(Rho*CL_max*S)).
V_max=183; %ft/s
T_max=P_Available/V_max.
V_min = sqrt(((T_max/W) * (Wing_Loading) - (Wing_Loading)*sqrt(((T_max/W)^2) -
(4*CD_Knot*K)))/(Rho*CD_Knot));
% For results verification v_min should be less than V_stall
%Climb performance of Super mushak
% Expression for Velocity at which maximum climb angle occurs is given by:
P_W=P_Available/W.
V_theta_max= (4*(Wing_Loading) *K)/(Rho*npr*P_W).

% calculating the maximum climb angle theta_max
Theta_max=asind(((P_Available)/(V_theta_max*W))-
((0.5)*(Rho)*(V_theta_max^2)*(Wing_Loading^-1)*(CD_Knot))-
((Wing_Loading)*((2*K)/(Rho*(V_theta_max^2)))));

% velocity at which R/C max will occur for a propeller-driven aircraft
% isgiven by
V_R_C_max=sqrt((2/Rho) * (((K)/((3)*(CD_Knot)))^0.5)*(Wing_Loading));
R_C_max=(P_Available/W) - ((V_R_C_max)*((1.155)/(L_D_max)));

%Hodograph
Thrust=(npr*P_Available). /Vel.

T_W=Thrust/W.

Vertical_velocity=Vel.*((T_W) - (0.5*Rho. *(Vel.^2).*(Wing_Loading)^-1*CD_Knot)-
(Wing_Loading*2*K./ (Rho*(Vel.^2))));

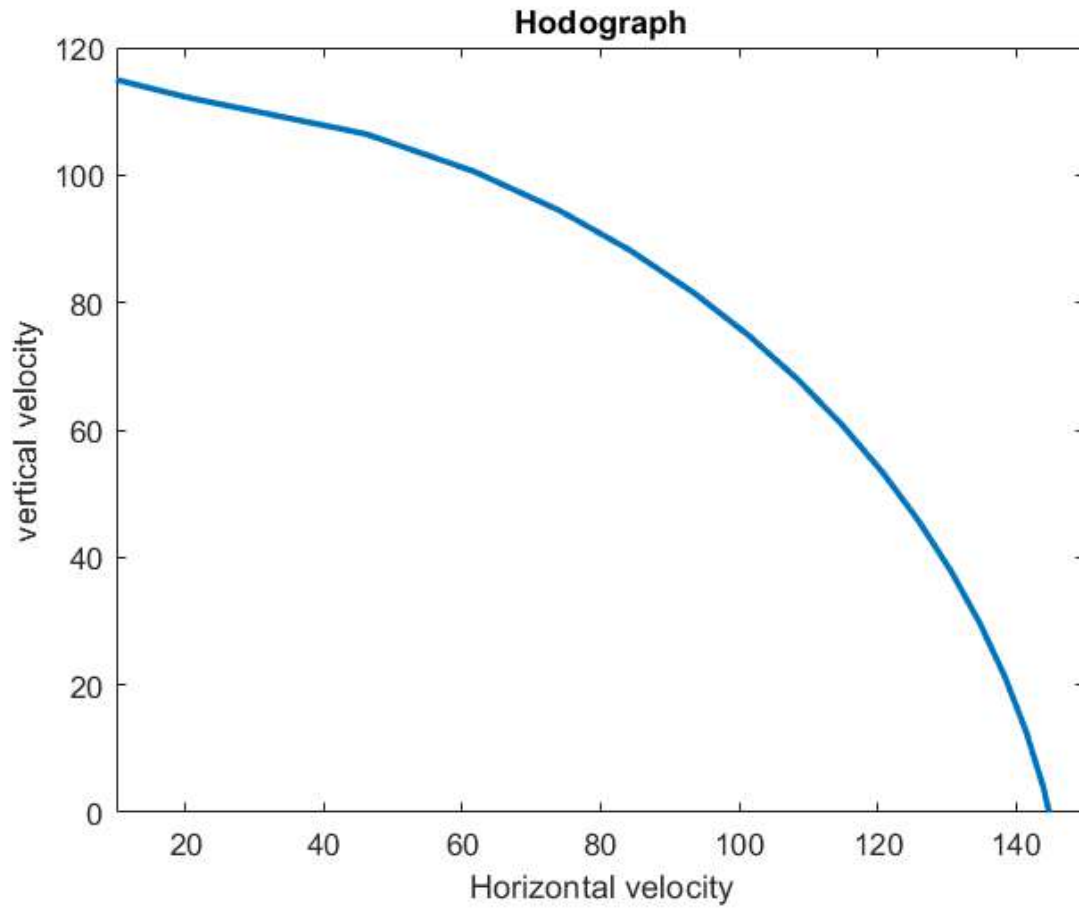
thetal=asind (Vertical_velocity. /Vel);

Horizontal_velocity=Vel.*(cosd(thetal)).

plot (Horizontal_velocity, Vertical_velocity,'m')
xlabel ('Horizontal velocity')
ylabel ('vertical velocity')
title('Hodograph')

```

Warning: Imaginary parts of complex X and/or Y arguments ignored.



```

%Glide (Unpowered) Flight
theta_min_Glide=atan(1/L_D_max).

% velocity for min glide occurs at velocity of CL by Cd max
V_theta_min_glide=V_CL_CD_max.
Altitude=450; % feet

Rho_450ft=0.002237.
min_glide_angle = atand(1/(CL_by_CD_max)).
V_min_glide_angle = V_CL_CD_max.

GlideRange = Altitude/tand(min_glide_angle).

GlideRange_miles = GlideRange/5280.

Vv_min_glide_angle = V_min_glide_angle * sind(min_glide_angle).

min_sink_rate = sqrt((2*Wing_Loading)/(Rho_450ft*(CL_3_2_CD_max) ^2));
V_min_sink_rate = V_CL_3_2_CD_max.

min_sink_rate_glide_angle = asind(min_sink_rate/V_min_sink_rate).

t_glide = 450/min_sink_rate.

glide_descent=-1*sqrt((2*Wing_Loading) . / (Rho*(CL_3_2_by_CD).^2));

plot (Vel,glide_descent,'c')
title ('Glide Descent')
xlabel ('velocity')

```

```
ylabel ('Descent Glide Rate')
```

